NACA TN 3645

# NATIONAL ADVISORY COMMITTEE FOR AERONAUTICS

**TECHNICAL NOTE 3645**

# WIND-TUNNEL INVESTIGATION OF EFFECTS OF FUSELAGE CROSS-SECTIONAL SHAPE, FUSELAGE BEND, AND VERTICAL-TAIL SIZE ON DIRECTIONAL CHARACTERISTICS OF NONOVERLAP-TYPE HELICOPTER FUSELAGE MODELS WITHOUT ROTORS

By James L. Williams

Langley Aeronautical Laboratory
Langley Field, Va.

Washington
March 1956

NATIONAL ADVISORY COMMITTEE FOR AERONAUTICS

TECHNICAL NOTE 3645

# WIND-TUNNEL INVESTIGATION OF EFFECTS OF FUSELAGE CROSS-SECTIONAL SHAPE, FUSELAGE BEND, AND VERTICAL-TAIL SIZE ON DIRECTIONAL CHARACTERISTICS OF NONOVERLAP-TYPE HELICOPTER FUSELAGE MODELS WITHOUT ROTORS

By James L. Williams

## SUMMARY

A low-speed investigation was made in the Langley stability tunnel to determine the directional stability characteristics of tandem nonoverlap-type helicopter fuselages without rotors. The investigation consisted of a study of both bent and straight fuselages having either circular or essentially elliptical cross sections and with two vertical-tail sizes.

The results of this investigation indicate that a straight fuselage with circular cross sections, in general, had a more nearly linear variation of yawing-moment coefficient with angle of sideslip and a smaller variation of directional stability with angle of attack than the bent and straight fuselage models with elliptical cross sections and a bent fuselage with a circular cross section. Changing the cross-sectional shape from elliptical to circular resulted in a more nearly linear variation of yawing-moment coefficient with angle of sideslip and a smaller variation of directional stability with angle of attack. Adding the bend in the fuselage, in general, made the adverse effects of flattening the fuselage cross section more pronounced. The basic twin vertical tails, each having an area of 46.30 square inches, did not provide directional stability throughout the angle-of-attack range for any of the models investigated; however, twin vertical tails of about $2\frac{1}{4}$ times this area provided a substantial improvement in the directional stability for all models.

## INTRODUCTION

The results of flight tests have shown that a tandem nonoverlap type of helicopter (a helicopter with nonoverlapping rotors) with a bent-fuselage form and a relatively deep elliptical nose section was directionally unstable at positive angles of attack and that this instability

was particularly undesirable in the autorotative and partial-power-descent flight conditions (ref. 1). A wind-tunnel investigation (ref. 2) of a model of this helicopter configuration, without rotors, has shown that the directional stability of the fuselage varied a large amount with angle of attack and that this variation of directional stability was associated with the rate of change with sideslip angle of an asymmetric trailing vortex system that existed on the fuselage. These characteristics are not commonly encountered with straight, relatively circular fuselages used for airplanes.

The use of spoilers around the nose of the fuselage resulted in an improvement in the directional stability characteristics of this configuration by reducing the unstable yawing moment obtained with the fuselage alone. These spoilers, of course, resulted in an increase in drag.

Since the bend in the fuselage of the nonoverlap-type helicopter may be necessary for rotor and ground clearance, an experimental investigation was made in the Langley stability tunnel in order to determine the relative influence of the fuselage cross-sectional shape and fuselage bend on the directional stability characteristics. As in the investigation of reference 2, these models were tested without rotors.

The present investigation consisted in the measurements of the aerodynamic forces and moments throughout a range of sideslip angles at four angles of attack for the models both without tails and with two sizes of twin vertical tails. The fuselage models used in this investigation were: a bent fuselage (fuselage 3 of ref. 2), a straight fuselage with essentially elliptical cross section at the nose, and both a bent fuselage and a straight fuselage with circular cross sections. All fuselages had, in general, the same longitudinal distribution of cross-sectional area.

## SYMBOLS

The data presented herein are referred to the wind system of axes with the origin at the assumed centers of gravity of the fuselages. The positive directions of forces, moments, and angles are shown in figure 1. The symbols and coefficients employed are defined as follows:

| | |
|---|---|
| $A$ | vertical-tail aspect ratio, $b^2/S_t$ |
| $b$ | vertical-tail height, ft |
| $\bar{c}_t$ | vertical-tail mean aerodynamic chord, ft |

| | |
|---|---|
| $c_t$ | vertical-tail chord, ft |
| $d$ | distance between vertical tails, ft |
| $l$ | distance between rotor hub centers, 4.23 ft |
| $l_t$ | tail length (distance from center of gravity to $c_t/4$ of vertical tail measured parallel to fuselage reference line), ft |
| $2S_d$ | total rotor disk area, 26.39 sq ft |
| $S_t$ | area of one vertical tail, sq ft |
| $t$ | tail thickness, ft (see fig. 3) |
| $V$ | free-stream velocity, ft/sec |
| $q$ | dynamic pressure, $\frac{\rho V^2}{2}$, lb/sq ft |
| $\rho$ | mass density of air, slugs/cu ft |
| $\alpha$ | angle of attack of fuselage reference line, deg |
| $\beta$ | angle of sideslip, deg |
| $\lambda_t$ | vertical-tail taper ratio |
| $C_D$ | drag coefficient, $\frac{\text{Drag}}{q2S_d}$ |
| $C_Y$ | side-force coefficient, $\frac{\text{Side force}}{q2S_d}$ |
| $C_n$ | yawing-moment coefficient, $\frac{\text{Yawing moment}}{q2S_d l}$ |
| $C_{n,t}$ | yawing-moment coefficient attributable to vertical tail |

$C_l$ rolling-moment coefficient, $\frac{\text{Rolling moment}}{q_2 S_d l}$

$C_{n_\beta} = \frac{\partial C_n}{\partial \beta}$ (slope of $C_n$ through $\beta = 0^\circ$)

$C_{n_{\beta,t}} = \left(C_{n_\beta} \text{ for fuselage with tail}\right) - \left(C_{n_\beta} \text{ for the fuselage alone}\right)$

Component designations:

$T_1$ tail 1 (tail 5 of ref. 2), (see fig. 3)

$T_2$ tail 2 (see fig. 3)

$F_1, F_2, F_3, F_4$ fuselages 1, 2, 3, and 4, respectively (see fig. 2)

## MODELS, APPARATUS, AND TESTS

The nonoverlap-type helicopter fuselage models used in this investigation were made of laminated mahogany and are shown in figure 2. These models are designated herein as:

$F_1$, bent fuselage with basic cross section referred to hereinafter as elliptical

$F_2$, bent fuselage with circular cross section

$F_3$, straight fuselage with elliptical cross section

$F_4$, straight fuselage with circular cross section

Each fuselage had the same cross-sectional shape (either circular or elliptical) throughout with the exception of fuselage $F_1$ where the elliptical section becomes somewhat distorted rearward of the center of gravity. All fuselages had approximately the same longitudinal distribution of cross-sectional area. These fuselages were the same length as fuselage 3 of reference 2 which was a 1/10-scale model of a present-day tandem-helicopter fuselage. The vertical tails $T_1$ and $T_2$ (fig. 3) used in the present tests were made of 1/4-inch-thick plywood ($T_2$ had

approximately $2\frac{1}{4}$ times the area of $T_1$). Photographs of the test fuselages with $T_1$ are presented as figure 4. Configuration $F_3T_2$ is shown mounted on a support strut in figure 5.

The models were mounted rigidly to a single strut support, at a point midway between the rotor hubs, in the 6-by 6-foot square test section of the Langley stability tunnel. The forces and moments were measured by means of a six-component mechanical balance system.

Except for a few cases, all tests were made at a dynamic pressure of 39.7 pounds per square foot which corresponds to a Mach number of about 0.17. The test Reynolds number was $5.50 \times 10^6$ based on the overall fuselage length. Three tests with the $F_2T_2$ configuration were made at a dynamic pressure of 24.9 pounds per square foot which corresponds to a Mach number of about 0.13 and a Reynolds number of $4.36 \times 10^6$. The angles of sideslip investigated for all configurations ranged from about $-25^\circ$ to $25^\circ$ at angles of attack of $-30^\circ$, $-10^\circ$, $10^\circ$, and $30^\circ$. The horizontal tail was set at an angle of incidence of approximately $9^\circ$ for all tail-on tests.

## CORRECTIONS

The data obtained in this investigation were not corrected for support-strut interference or blockage effects with the exception of the drag coefficient, which was corrected only for tares. In general, previous tests have indicated that these corrections are not important to the interpretation of these results.

## RESULTS AND DISCUSSION

### Presentation of Data

The basic data in the form of yawing-moment coefficients plotted against $\beta$ are presented in figure 6 for the fuselages with tail 1 ($T_1$), in figure 7 for the fuselages alone, in figure 8 for the isolated tail ($T_1$) and the contribution of the tail to the yawing-moment coefficient, and in figure 9 for the fuselages with tail 2 ($T_2$). A plot of the directional stability parameter $C_{n_\beta}$ (measured through $\beta = 0^\circ$) against $\alpha$ for the fuselages alone and fuselages with $T_1$ and $T_2$ is presented as

figure 10. In figure 11 is presented the contribution of the tails to the directional stability as expressed by the yawing-moment coefficient of the fuselage-tail combination minus the yawing-moment coefficient of the fuselage. Also presented in figure 11 are experimental and calculated data for isolated tail $T_1$ and calculated data for $T_2$. The drag coefficient plotted against $\alpha$ is presented as figure 12 for the fuselages alone and for the fuselages with $T_1$. Since the purpose of the present paper is to provide an evaluation of the directional stability, only the yawing-moment data are discussed. The side-force and rolling-moment coefficients were also obtained, however, and are presented in figures 13 to 18 without discussion.

## Directional Characteristics of Fuselage With and Without $T_1$

Of all the configurations investigated, $F_4T_1$ (straight fuselage with circular cross section) has the most nearly linear yawing-moment characteristics (see fig. 6) and the smallest variation of $C_{n_\beta}$ (measured through $\beta = 0^\circ$) with angle of attack (see fig. 10). Configuration $F_4T_1$ generally had about neutral stability for the angle-of-attack range investigated with the exception of $\alpha = 10^\circ$. These data indicate, to a large degree, that the vertical tail ($T_1$) is not of sufficient size to provide much directional stability.

An examination of the data for the remaining configurations $F_1T_1$, $F_2T_1$, and $F_3T_1$ (figs. 6 and 10) shows that, in general, $F_3T_1$ has better stability characteristics than either $F_2T_1$ or $F_1T_1$ since its directional stability varied, in comparison, only a small amount with angle of attack. The results for the bent-fuselage models ($F_2T_1$ and $F_1T_1$) show that the directional stability varied a large amount with angle of attack; however, the magnitude of this effect was smaller for $F_2T_1$ than for $F_1T_1$. (See figs. 6 and 10.)

The effect of cross-sectional shape on the yawing-moment characteristics for the bent and straight fuselages can be seen from a study of figures 6 and 10. These results show that, for the bent fuselages, changing from elliptical cross section to circular cross section generally resulted in a more nearly linear curve of $C_n$ with $\beta$ and less variation of $C_{n_\beta}$ with angle of attack. This effect of cross-sectional shape is similar to the results for airplane fuselages with a deep cross section. (See refs. 3 and 4.) Results for the straight fuselages with tail $T_1$ (figs. 6(c), 6(d), and 10) show generally a similar, although somewhat

smaller, effect of cross section. In general, the bend in the fuselage makes the adverse effect of flattening the fuselage cross section more pronounced. (See figs. 6 and 10.)

The results of figures 7 and 10 show, in general, that the effect of cross section and bend on the yawing-moment characteristics for the fuselages alone are similar to the results obtained for the complete model. The use of circular cross section $F_2$ instead of elliptical cross section $F_1$ for the bent fuselages resulted generally in a more nearly linear variation of $C_n$ with angle of sideslip $\beta$ and in a smaller variation of $C_{n_\beta}$ with angle of attack. These effects, however, were somewhat less for the straight fuselages $F_3$ and $F_4$. (See figs. 7 and 10.) A comparison of the data of fuselages $F_1$ and $F_3$ and fuselages $F_2$ and $F_4$ indicates that not only did the bend cause a less linear variation of $C_n$ with angle of sideslip and increase the variation of $C_{n_\beta}$ with angle of attack, but also the fuselage alone was directionally stable at certain angles of attack for a limited sideslip range which is not usually the case for a fuselage alone.

The results of figures 8 and 11 show that the vertical tail $T_1$, when mounted on any of the fuselages, is considerably affected by adverse fuselage sidewash, which generally results in a tail effectiveness considerably smaller at a given sideslip angle than that of the isolated-tail assembly. The sidewash effect probably causes the erratic variation of yawing-moment coefficient at large angles of sideslip for the complete model which is not generally present for the fuselages without tail. (Compare figs. 6 and 7.)

The $C_{n_{\beta,t}}$ results calculated with the aid of references 5 and 6 for the isolated tail (fig. 11) are in fair agreement with the measured results. The differences between calculated and measured data may be the result of failure to include the end-plate effect of the horizontal tail in the calculated isolated tail values.

## Directional Characteristics of Fuselage with Tail $T_2$

The effect of substituting $T_2$ (a tail with about $2\frac{1}{4}$ times the area of $T_1$) in place of $T_1$ can be seen by comparing the data of figures 6 and 9. As was expected, the tail $T_2$ resulted in a substantial improvement in the directional stability characteristics for all fuselage models; however, the erratic behavior of the yawing-moment-coefficient curves with angle of sideslip (fig. 9) was still apparent.

A study of the yawing-moment results of figures 6 and 9 and of the directional stability parameter $C_{n_\beta}$ for the configurations with $T_1$ or $T_2$ (fig. 10) and the corresponding contribution of $T_1$ and $T_2$ to the directional stability parameter $C_{n_{\beta,t}}$ (fig. 11) indicates that, except for magnitude, the effect of changing the fuselage cross section and the effect of bend when $T_2$ is used is similar to that for the fuselages with $T_1$.

## CONCLUSIONS

The results of a low-speed investigation in the Langley stability tunnel to determine the directional stability characteristics of nonoverlap-type tandem helicopter fuselage models has indicated the following conclusions:

1. A straight fuselage model with circular cross section, in general, had a more nearly linear variation of yawing-moment coefficient with angle of sideslip and a smaller variation of directional stability with angle of attack than bent and straight fuselage models with essentially elliptical cross section or than a bent fuselage with circular cross section.

2. Changing the fuselage cross-sectional shape from elliptical to circular cross section resulted in a more nearly linear variation of yawing-moment coefficient with angle of sideslip and in a smaller variation of directional stability with angle of attack. Adding the bend in the fuselage, in general, made the adverse effects of flattening the fuselage cross section more pronounced.

3. Twin vertical tails (each having an area of 46.30 square inches) did not provide directional stability throughout the angle-of-attack range for any of the models investigated; however, twin vertical tails of about $2\frac{1}{4}$ times this area provided a substantial improvement in the directional stability for all models.

Langley Aeronautical Laboratory,
National Advisory Committee for Aeronautics,
Langley Field, Va., January 19, 1956.

## REFERENCES

1. Amer, Kenneth B., and Tapscott, Robert J.: Studies of the Lateral-Directional Flying Qualities of a Tandem Helicopter in Forward Flight. NACA Rep. 1207, 1954. (Supersedes NACA TN 2984.)

2. Williams, James L.: Directional Stability Characteristics of Two Types of Tandem Helicopter Fuselage Models. NACA TN 3201, 1954.

3. Letko, William, and Williams, James L.: Experimental Investigation at Low Speed of Effects of Fuselage Cross Section on Static Longitudinal and Lateral Stability Characteristics of Models Having 0° and 45° Sweptback Surfaces. NACA TN 3551, 1955.

4. Bates, William R.: Static Stability of Fuselages Having a Relatively Flat Cross Section. NACA TN 3429, 1955. (Supersedes NACA RM L9I06a.)

5. DeYoung, John: Theoretical Additional Span Loading Characteristics of Wings With Arbitrary Sweep, Aspect Ratio, and Taper Ratio. NACA TN 1491, 1947.

6. Queijo, M. J., and Wolhart, Walter D.: Experimental Investigation of the Effect of Vertical-Tail Size and Length and of Fuselage Shape and Length on the Static Lateral Stability Characteristics of a Model With 45° Sweptback Wing and Tail Surfaces. NACA Rep. 1049, 1951. (Supersedes NACA TN 2168.)

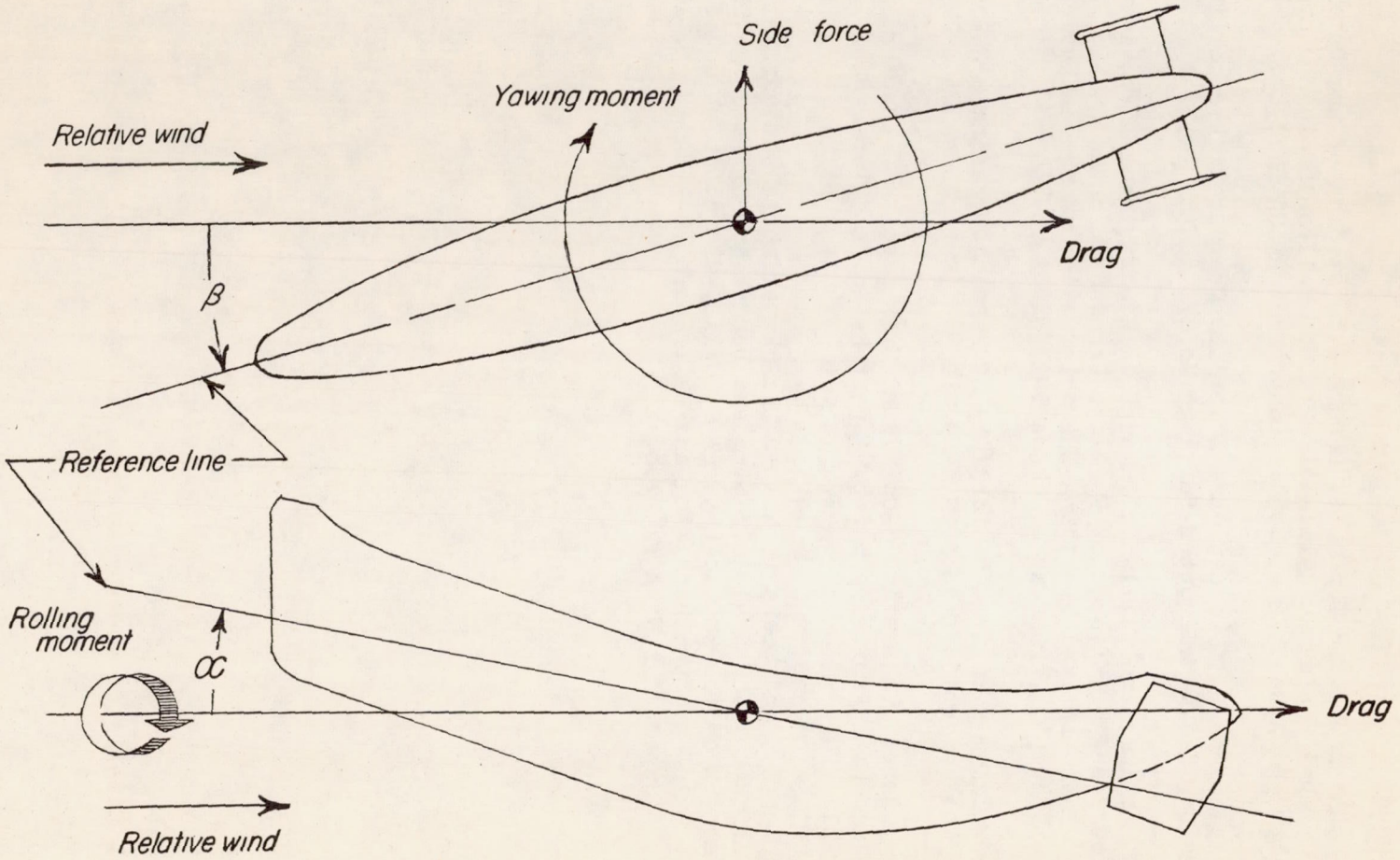


Figure 1.- System of wind axes. Arrows indicate positive direction of forces, moments, and angles.

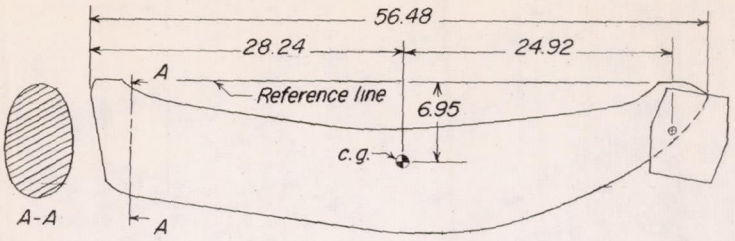


(a) Configuration $F_1T_1$.

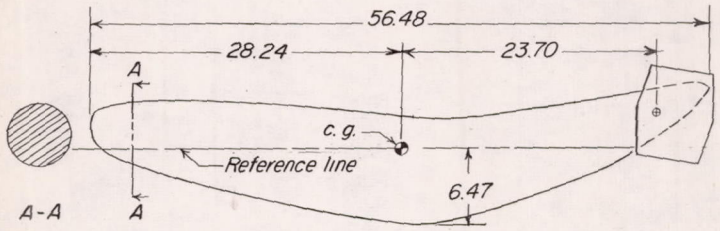


(b) Configuration $F_2T_1$.

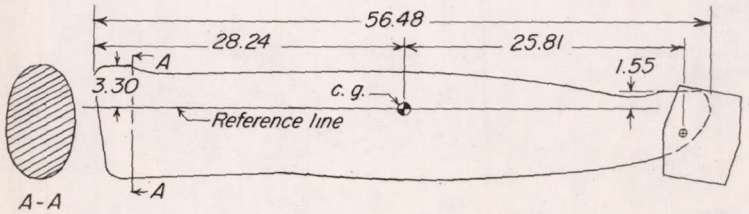


(c) Configuration $F_3T_1$.

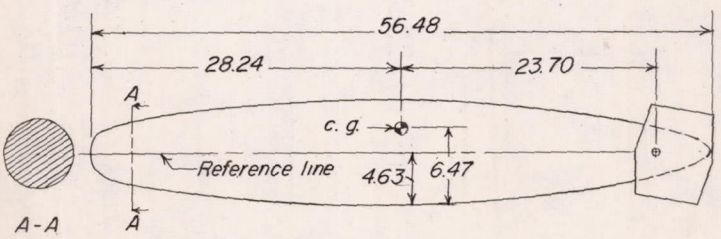


(d) Configuration $F_4T_1$.

Figure 2.- Details of nonoverlap-type fuselages. All dimensions are in inches.

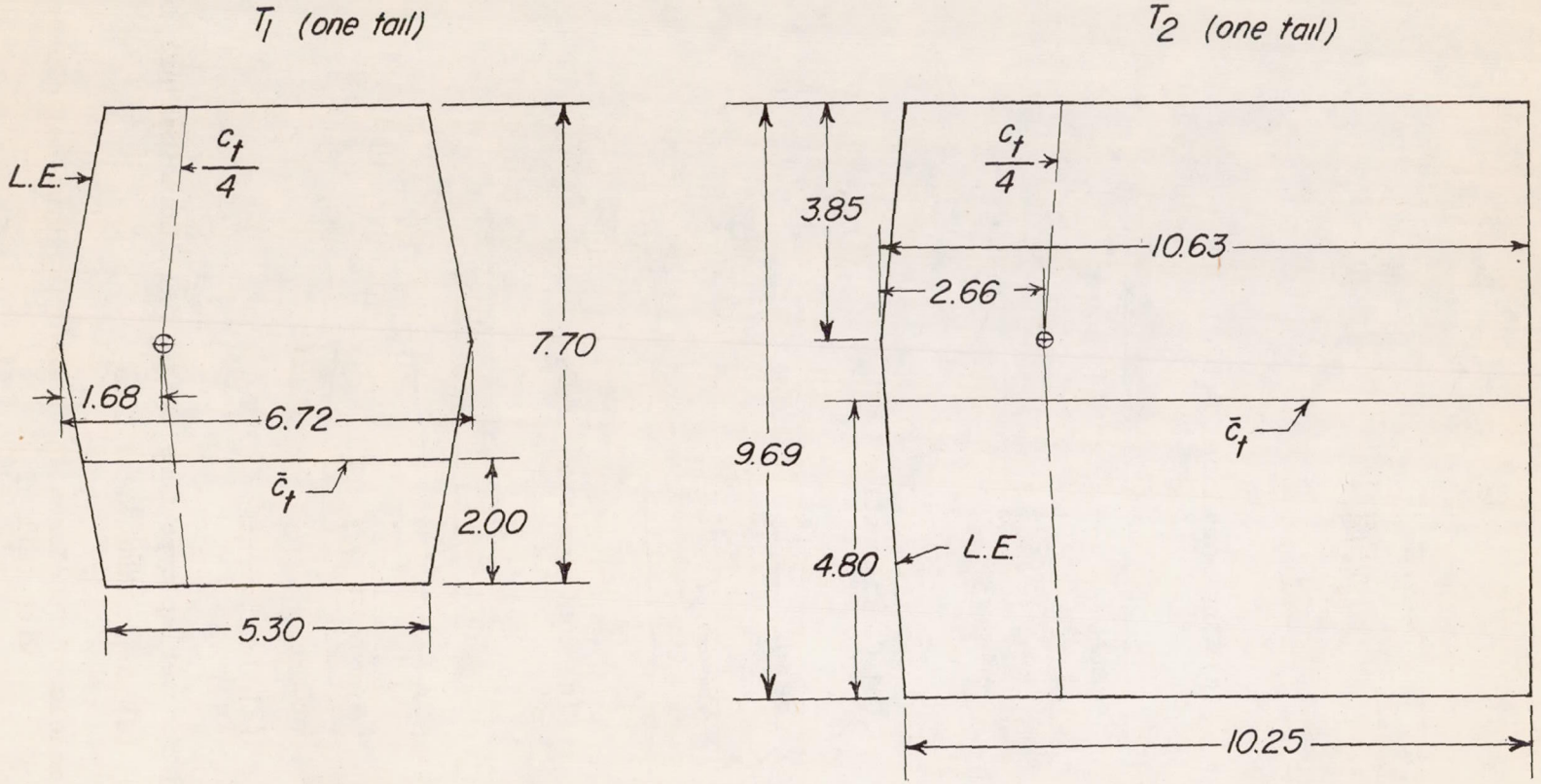


| | | |
|---|---|---|
| $A$ | 1.28 | .93 |
| $\bar{c}_t$ | 6.00 in. | 10.47 in. |
| $d$ | 10.00 in. | 10.00 in. |
| $S_t$ | 46.30 in.$^2$ | 101.40 in.$^2$ |
| $t$ | .25 in. | .25 in. |
| $\lambda_t$ | .79 | .97 |

$l_t$ (in.)

| | $F_1$ | $F_2$ | $F_3$ | $F_4$ |
|---|---|---|---|---|
| $T_1$ | 24.92 | 23.70 | 25.81 | 23.70 |
| $T_2$ | 26.05 | 24.83 | 26.80 | 24.83 |

Figure 3.- Vertical tails used in tests. All dimensions are in inches.

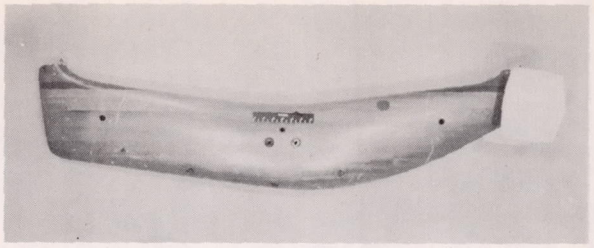

L-87048

(a) Configuration $F_1T_1$ (fuselage 3 of reference 2).

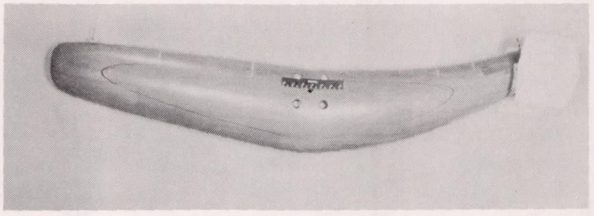

L-87049

(b) Configuration $F_2T_1$.

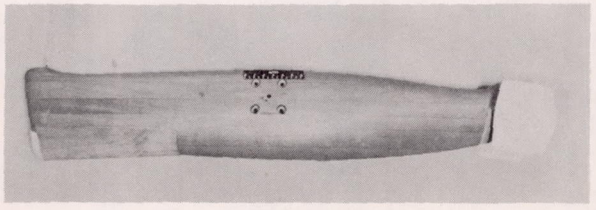

L-87047

(c) Configuration $F_3T_1$.

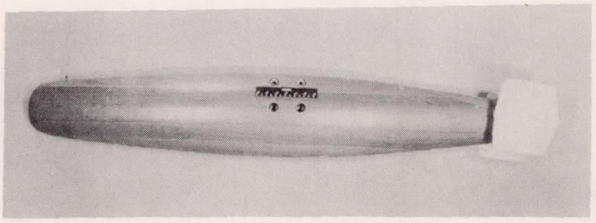

L-87050

(d) Configuration $F_4T_1$.

Figure 4.- Views of models of fuselages for nonoverlap-type helicopter with tail $T_1$.

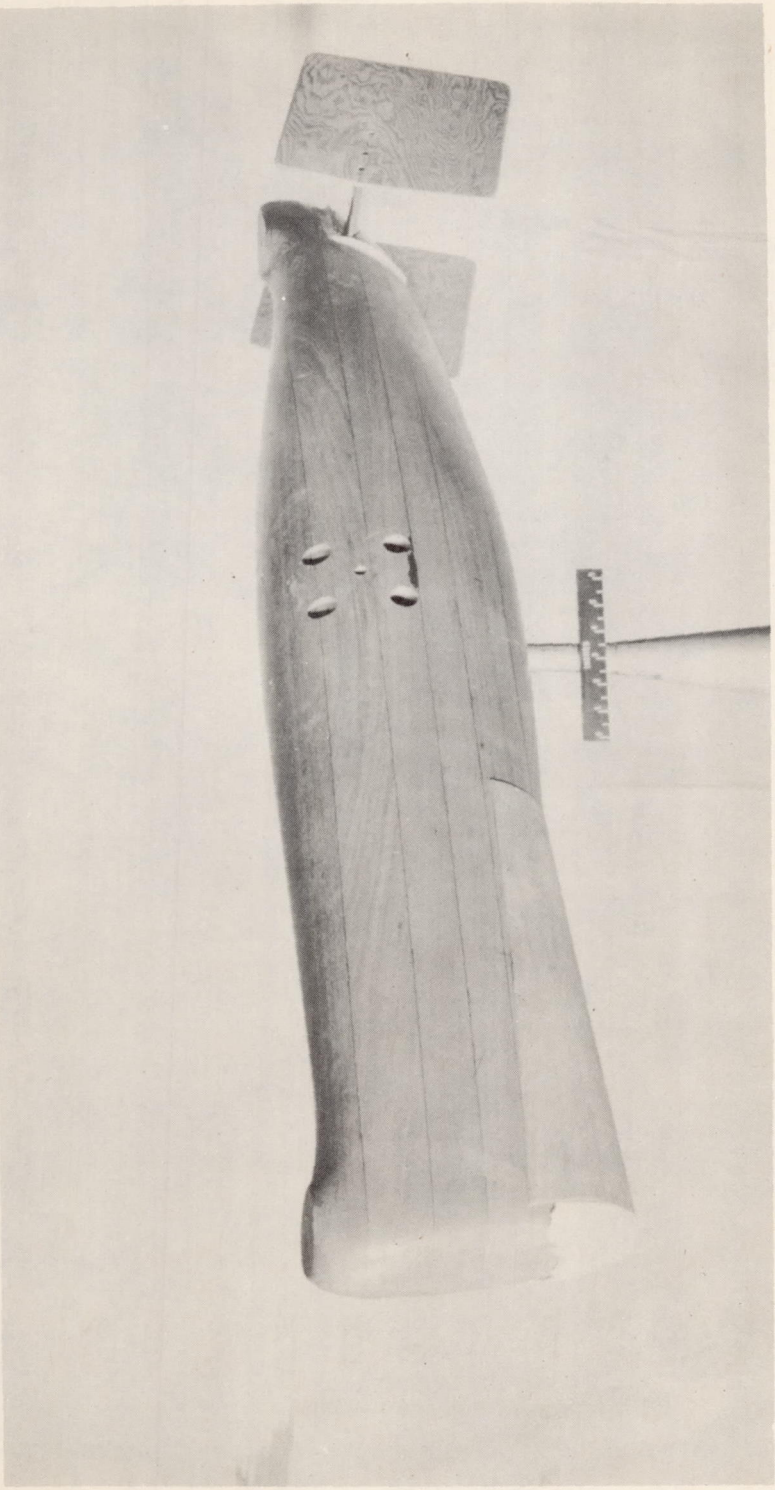

L-87052

Figure 5.- View of configuration $F_3T_2$.

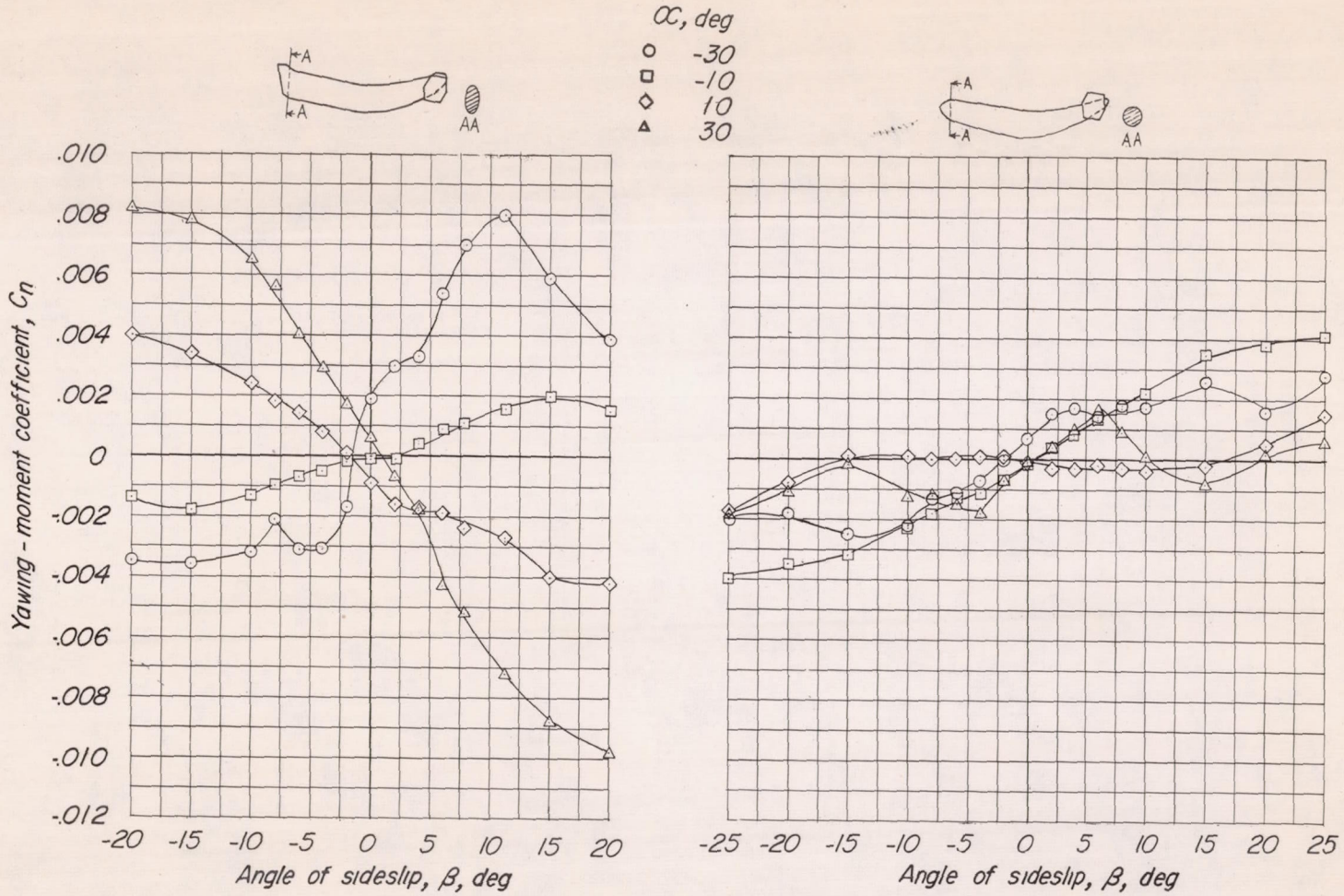


(a) Configuration $F_1T_1$.

(b) Configuration $F_2T_1$.

Figure 6.- Yawing-moment characteristics in sideslip at several angles of attack for various configurations of a nonoverlap-type helicopter fuselage model.

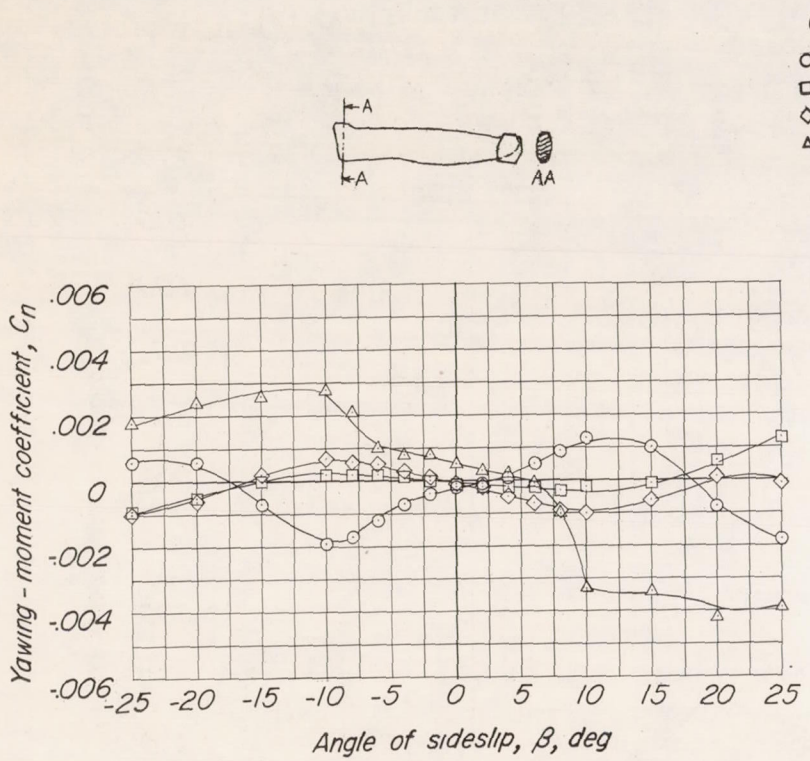


(c) Configuration $F_3T_1$.

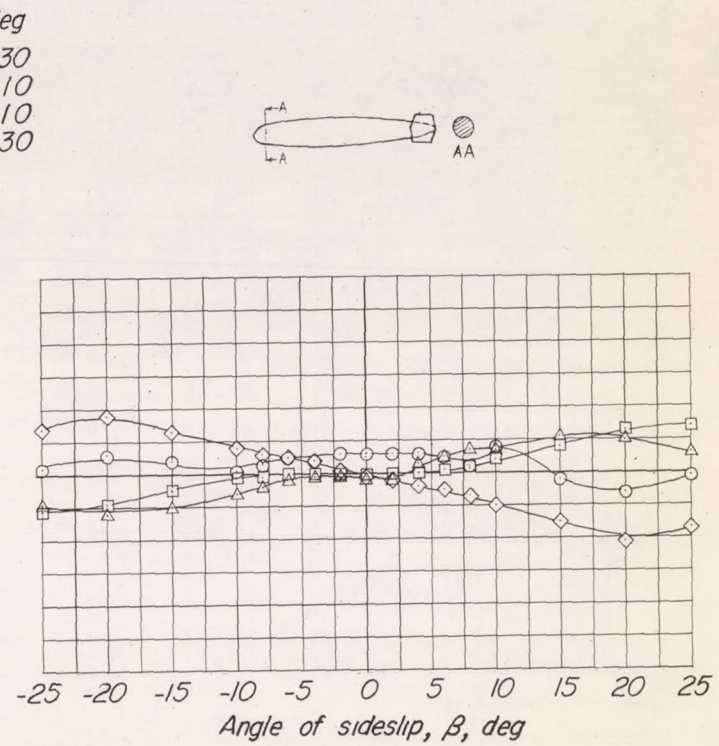


(d) Configuration $F_4T_1$.

Figure 6.- Concluded.

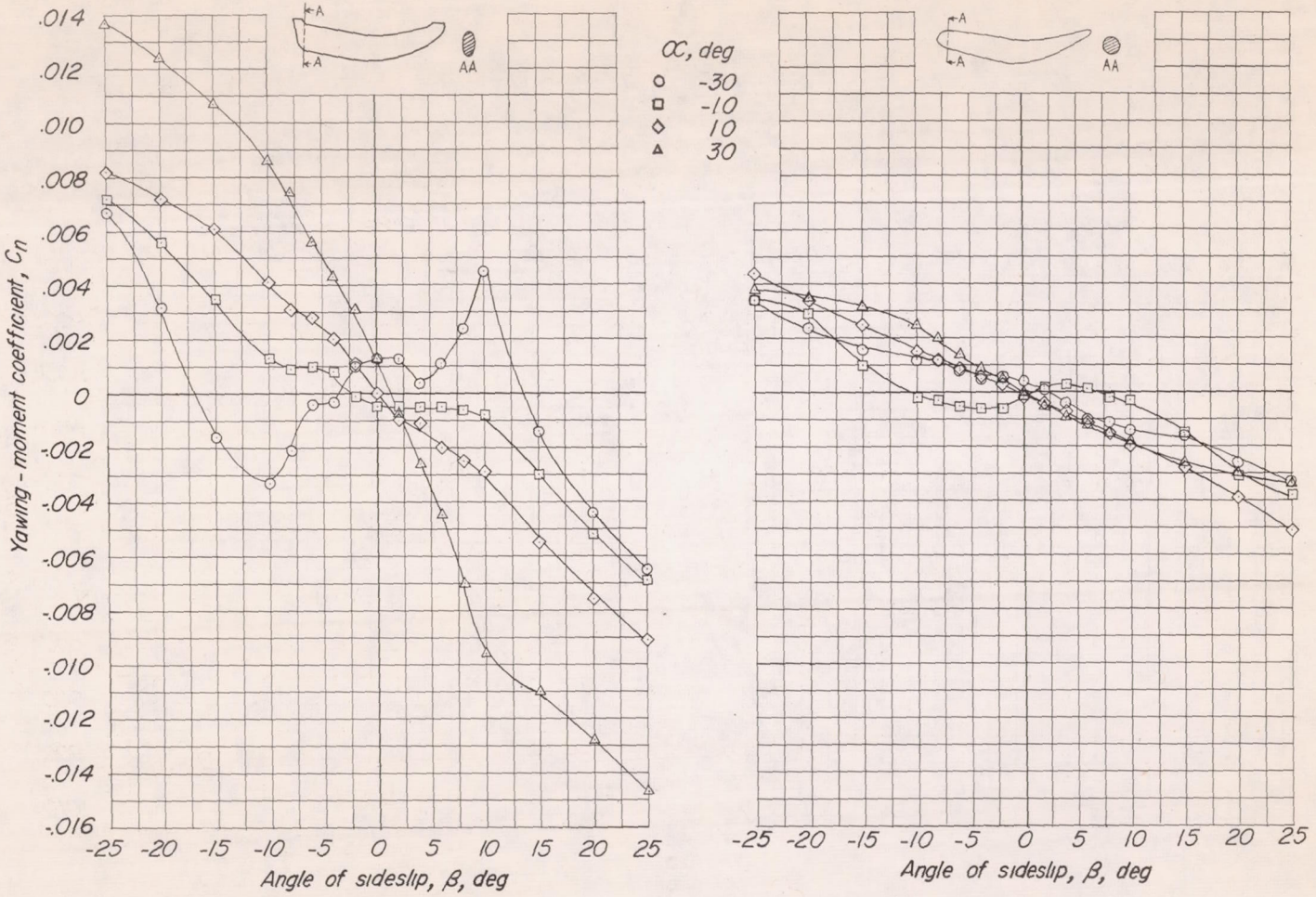


(a) Configuration $F_1$.

(b) Configuration $F_2$.

Figure 7.- Yawing-moment characteristics in sideslip at several angles of attack for various configurations of a nonoverlap-type helicopter fuselage model.

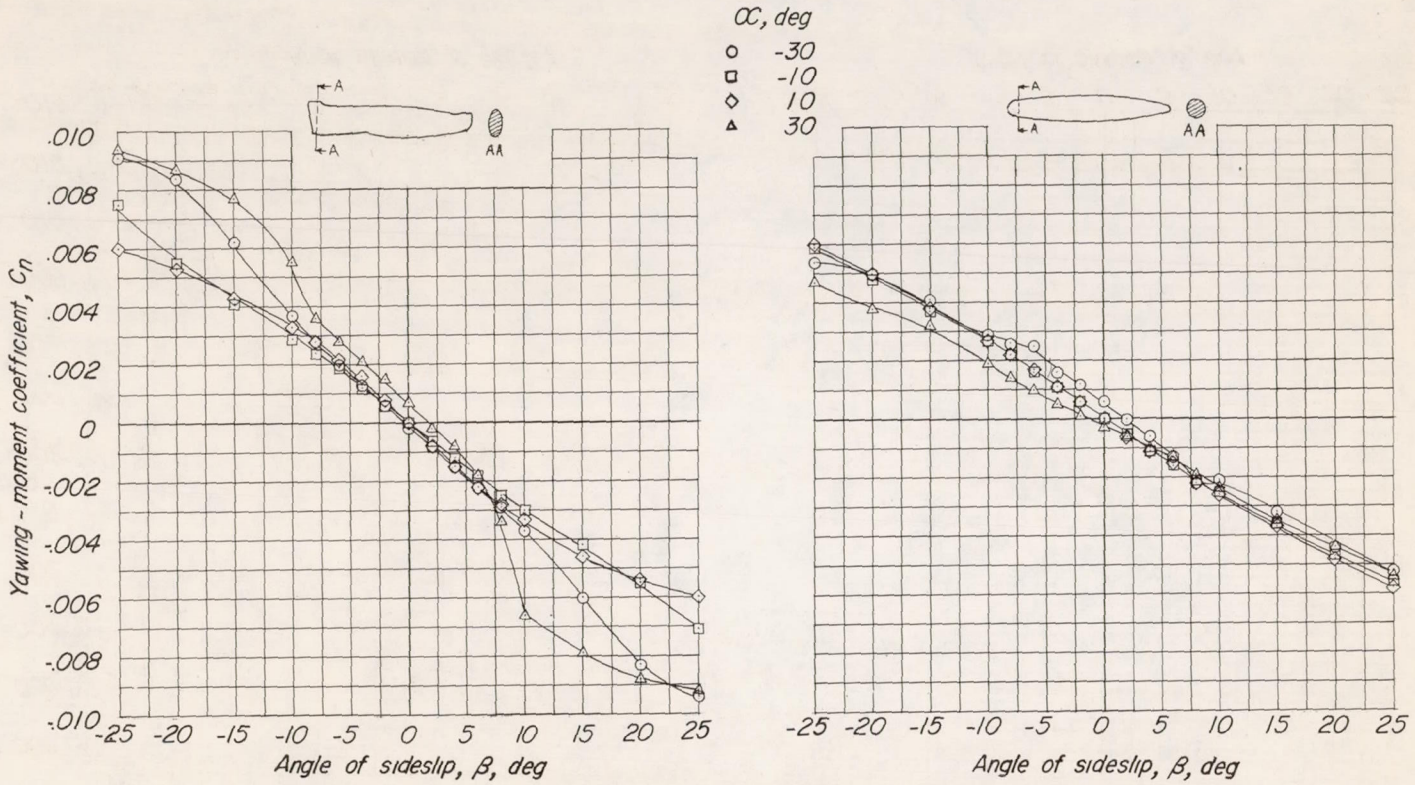


(c) Configuration $F_3$.

(d) Configuration $F_4$.

Figure 7.- Concluded.

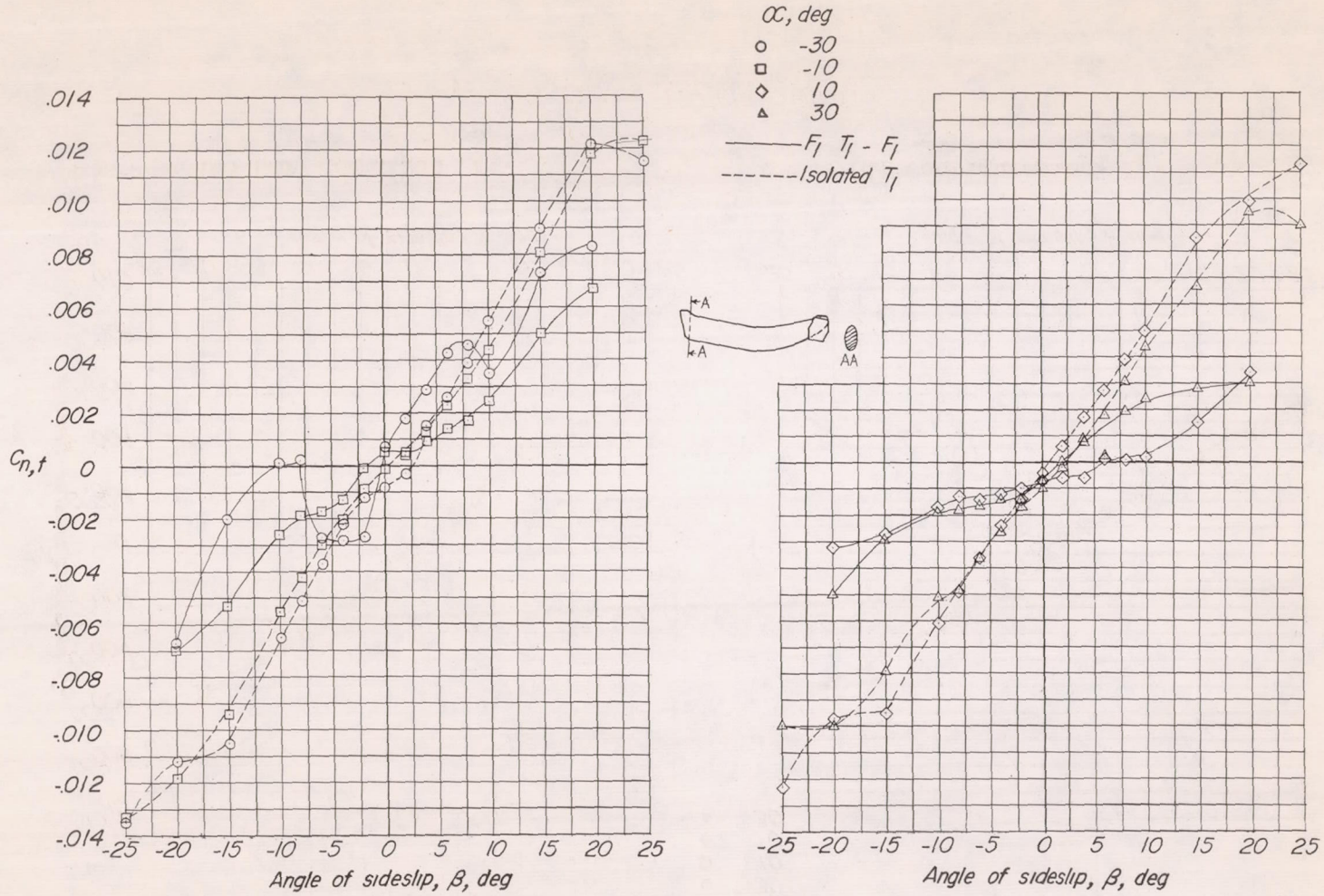


(a) Configuration $F_1$.

Figure 8.- Variation with sideslip angle of yawing moment of isolated tail and the tail contribution to the yawing moment at several angles of attack.

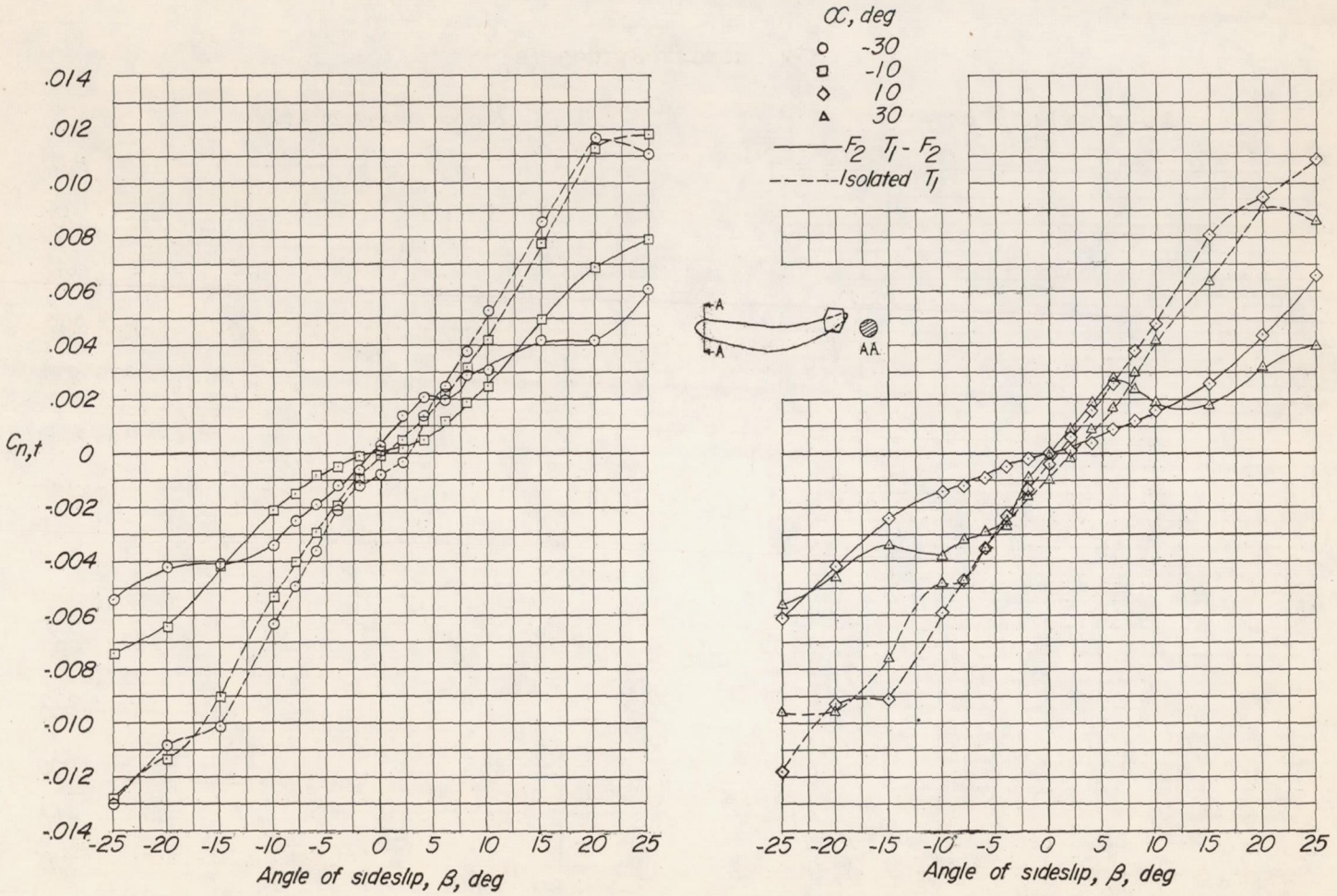


(b) Configuration $F_2$.

Figure 8.- Continued.

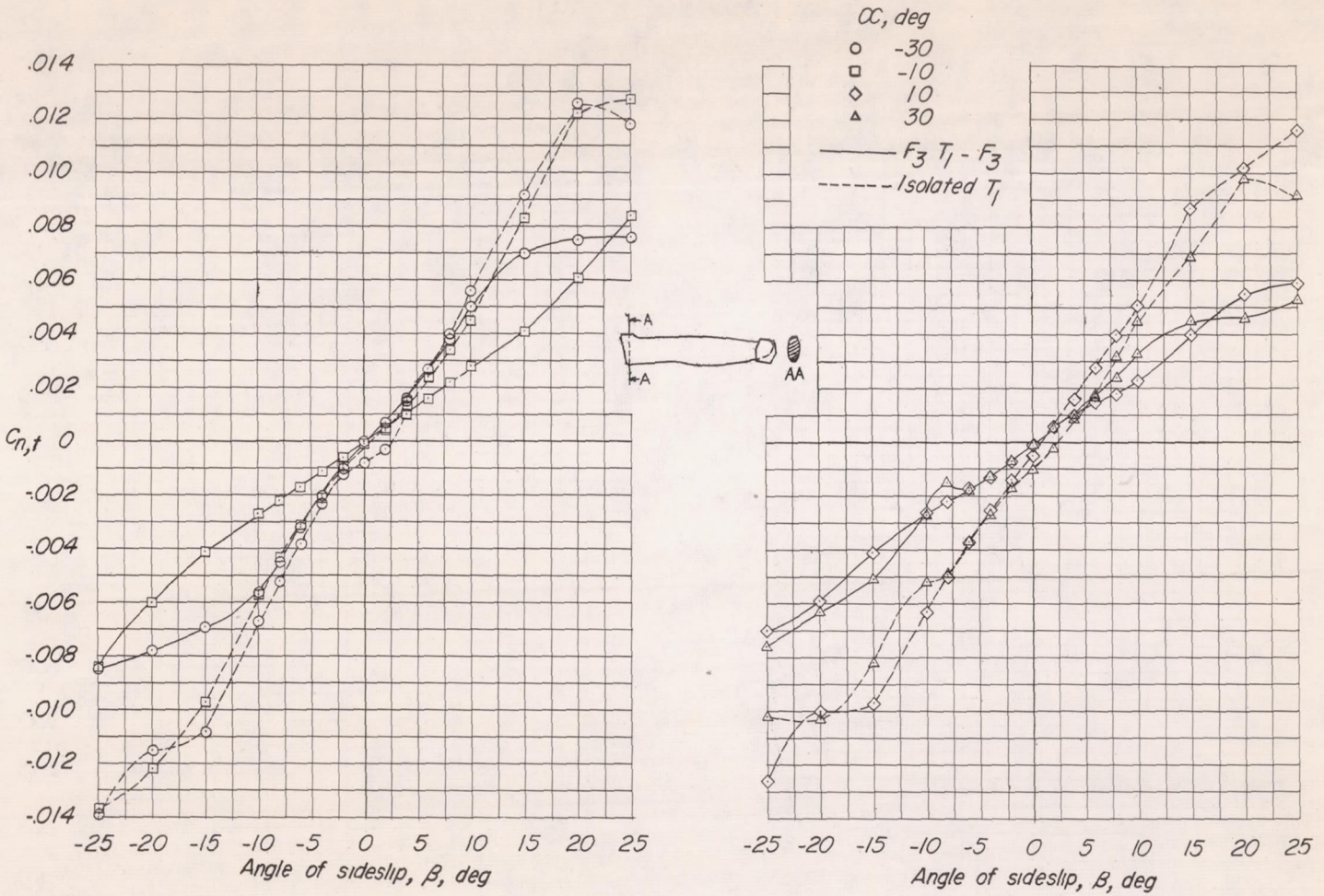


(c) Configuration $F_3$.

Figure 8.- Continued.

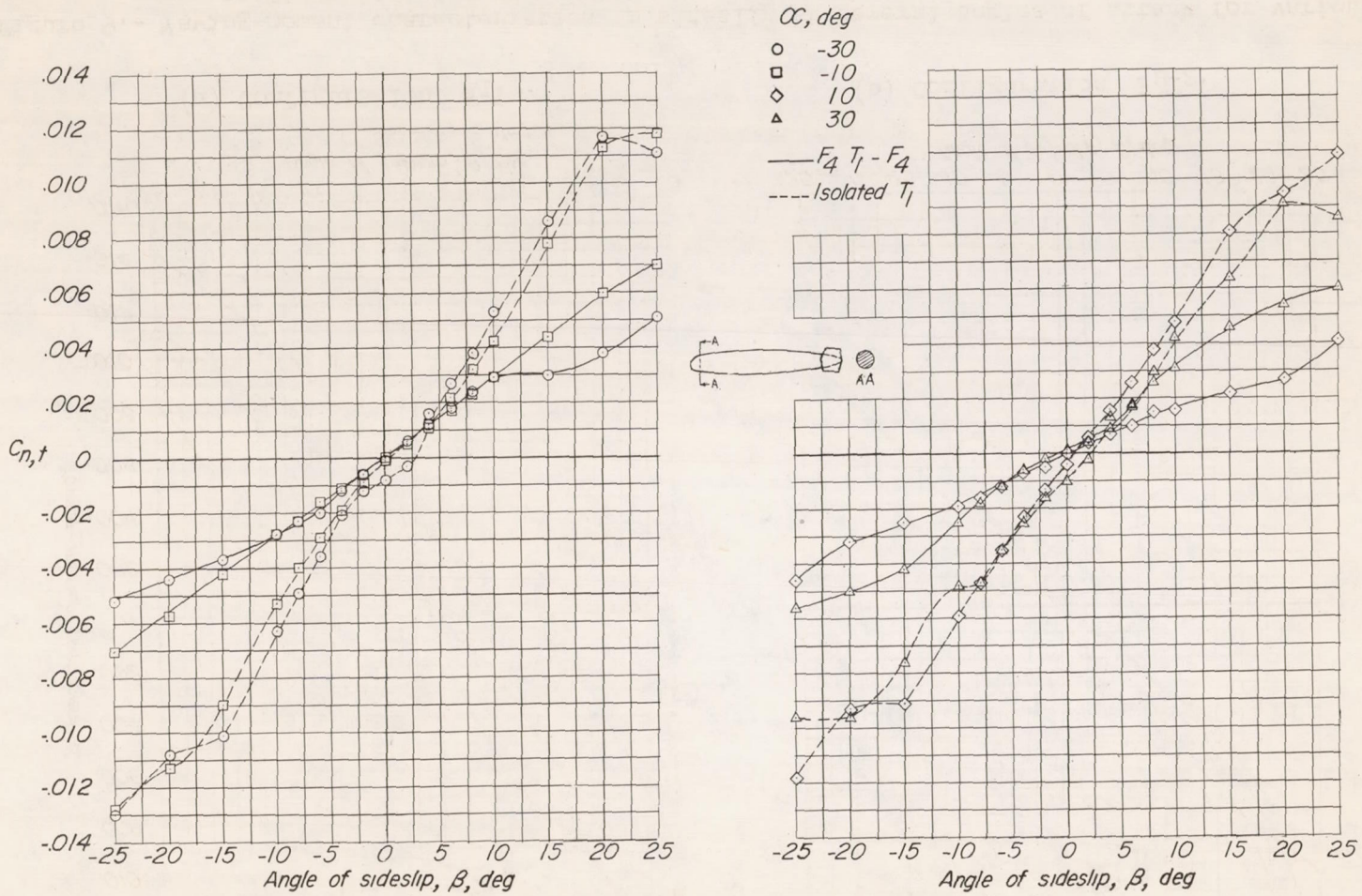


(d) Configuration $F_4$.

Figure 8.- Concluded.

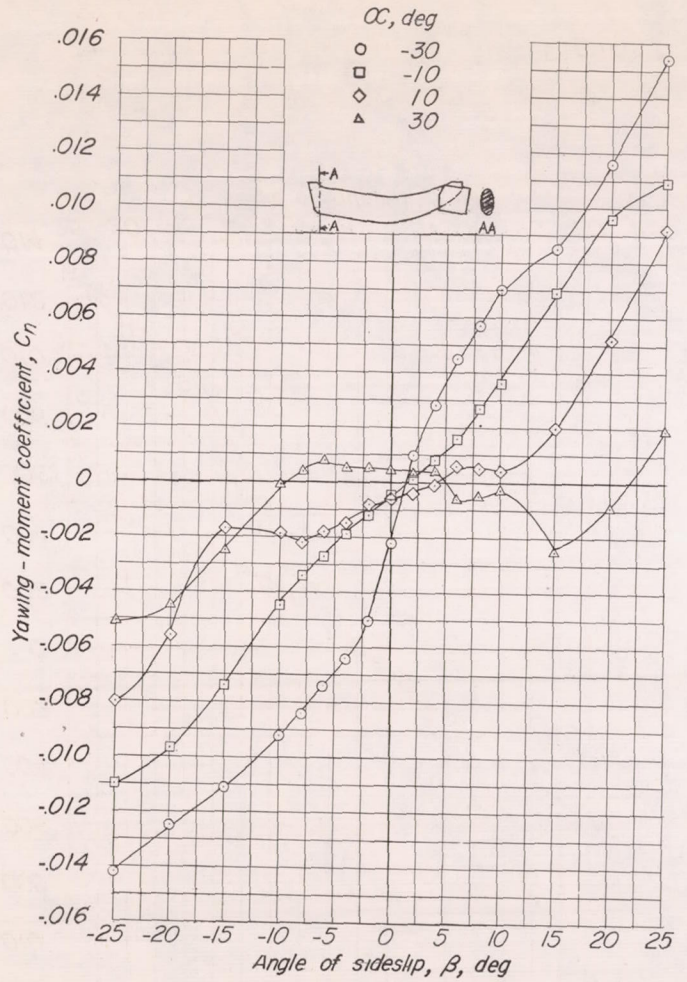


(a) Configuration $F_1T_2$.

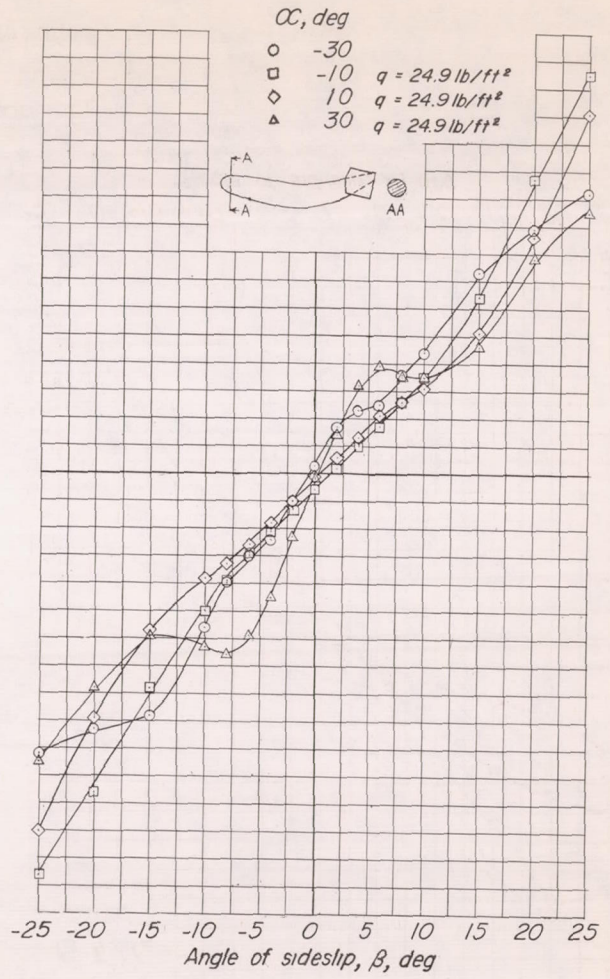


(b) Configuration $F_2T_2$.

Figure 9.- Yawing-moment characteristics in sideslip at several angles of attack for various configurations of a nonoverlap-type helicopter fuselage model.

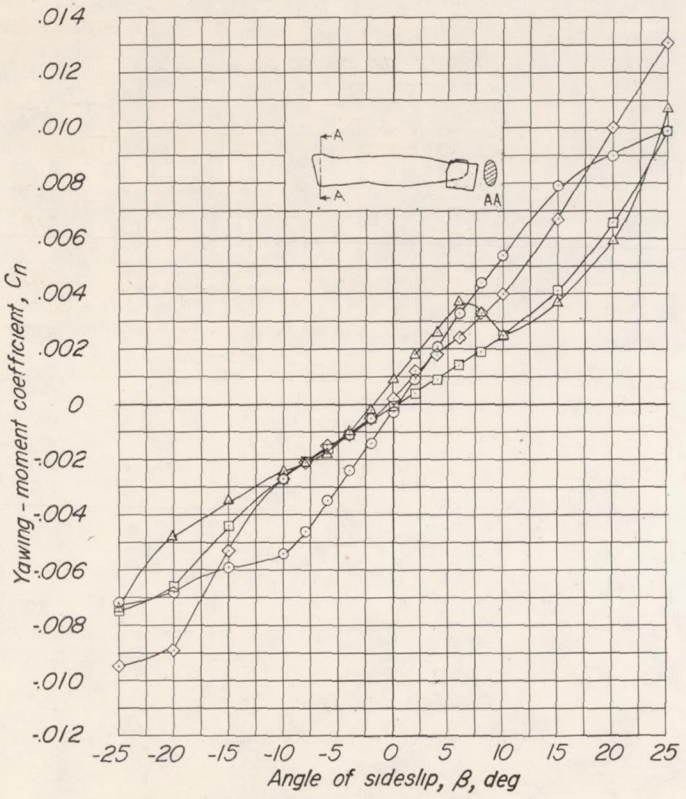


(c) Configuration $F_3T_2$.

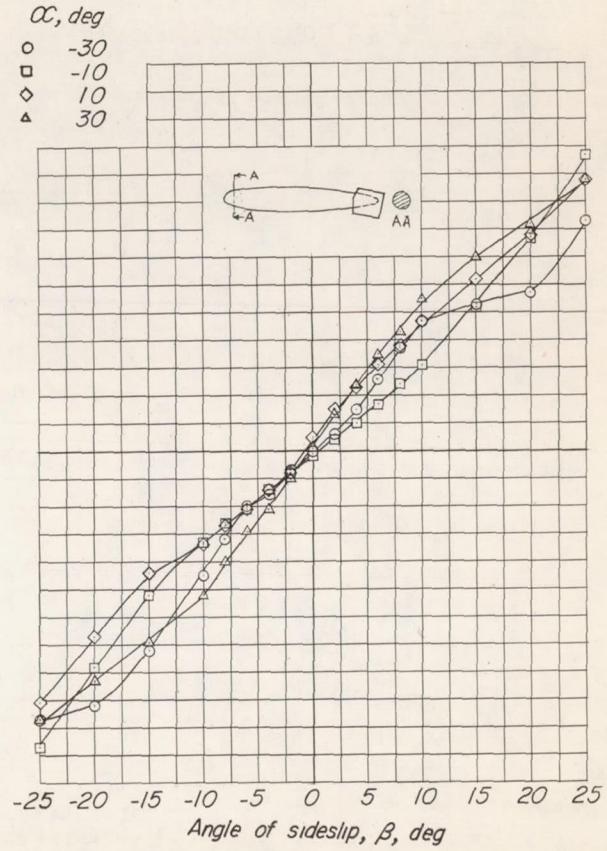


(d) Configuration $F_4T_2$.

Figure 9.- Concluded.

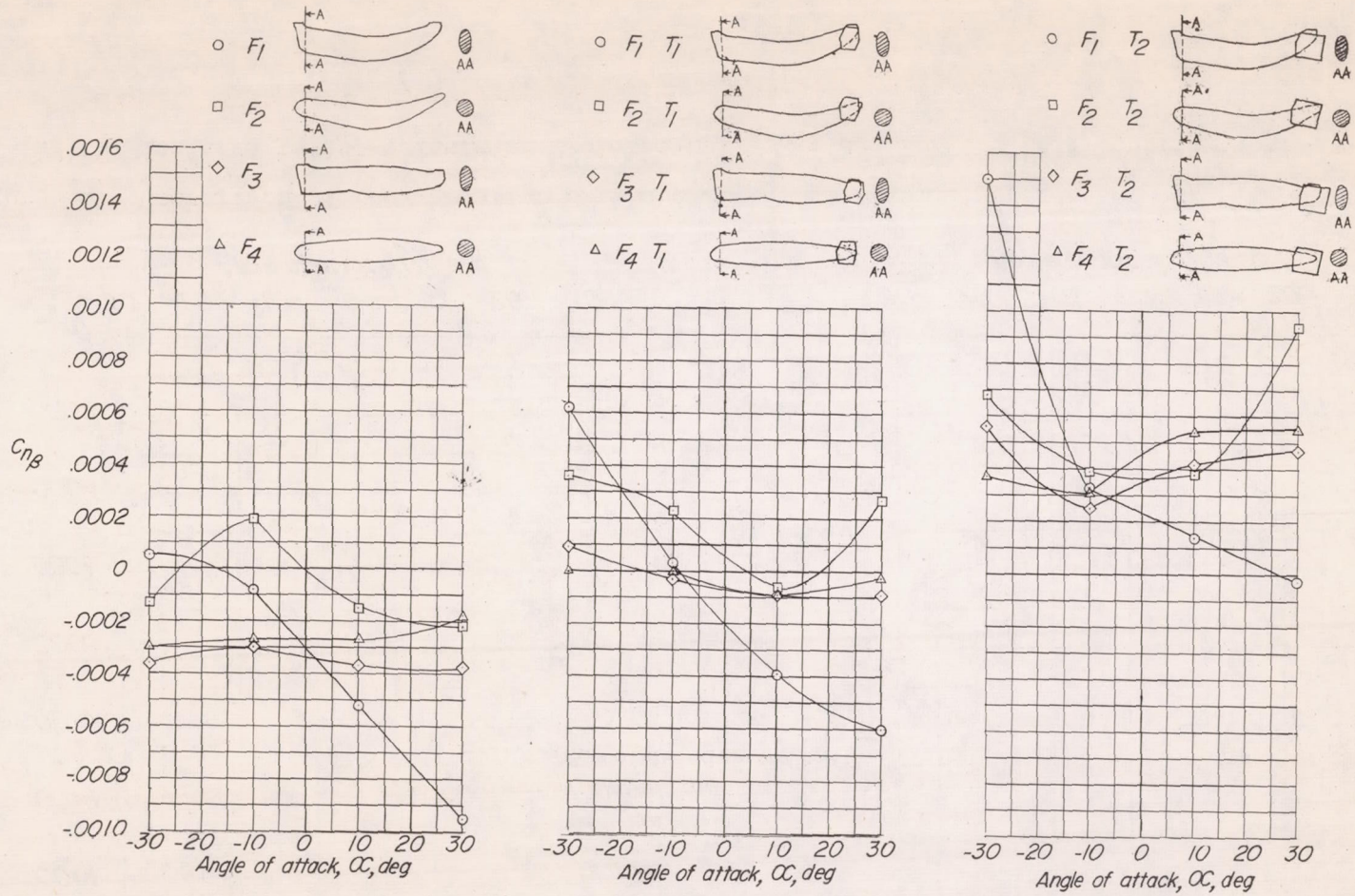


(a) Fuselage alone.

(b) Fuselage - $T_1$ configurations.

(c) Fuselage - $T_2$ configurations.

Figure 10.- Comparison of the variation of directional stability parameter $C_{n_\beta}$ ($\beta = 0^\circ$) with angle of attack for the fuselage models with and without $T_1$ and $T_2$.

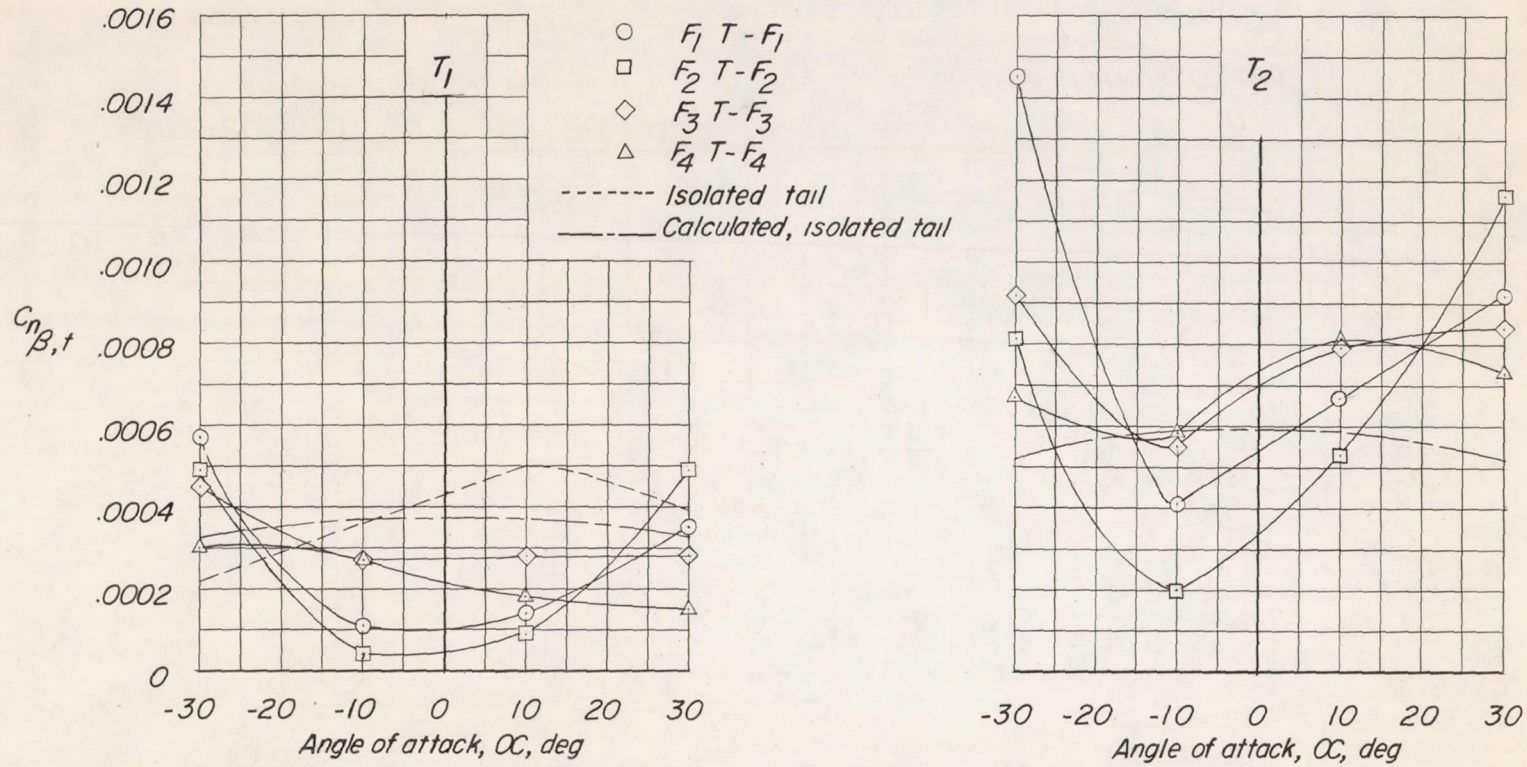


Figure 11.- Comparison of the variation of the directional stability parameter $C_{n_\beta}$ ($\beta = 0^\circ$) for the isolated tails, calculated isolated tail $T_1$, and for the tail contribution.

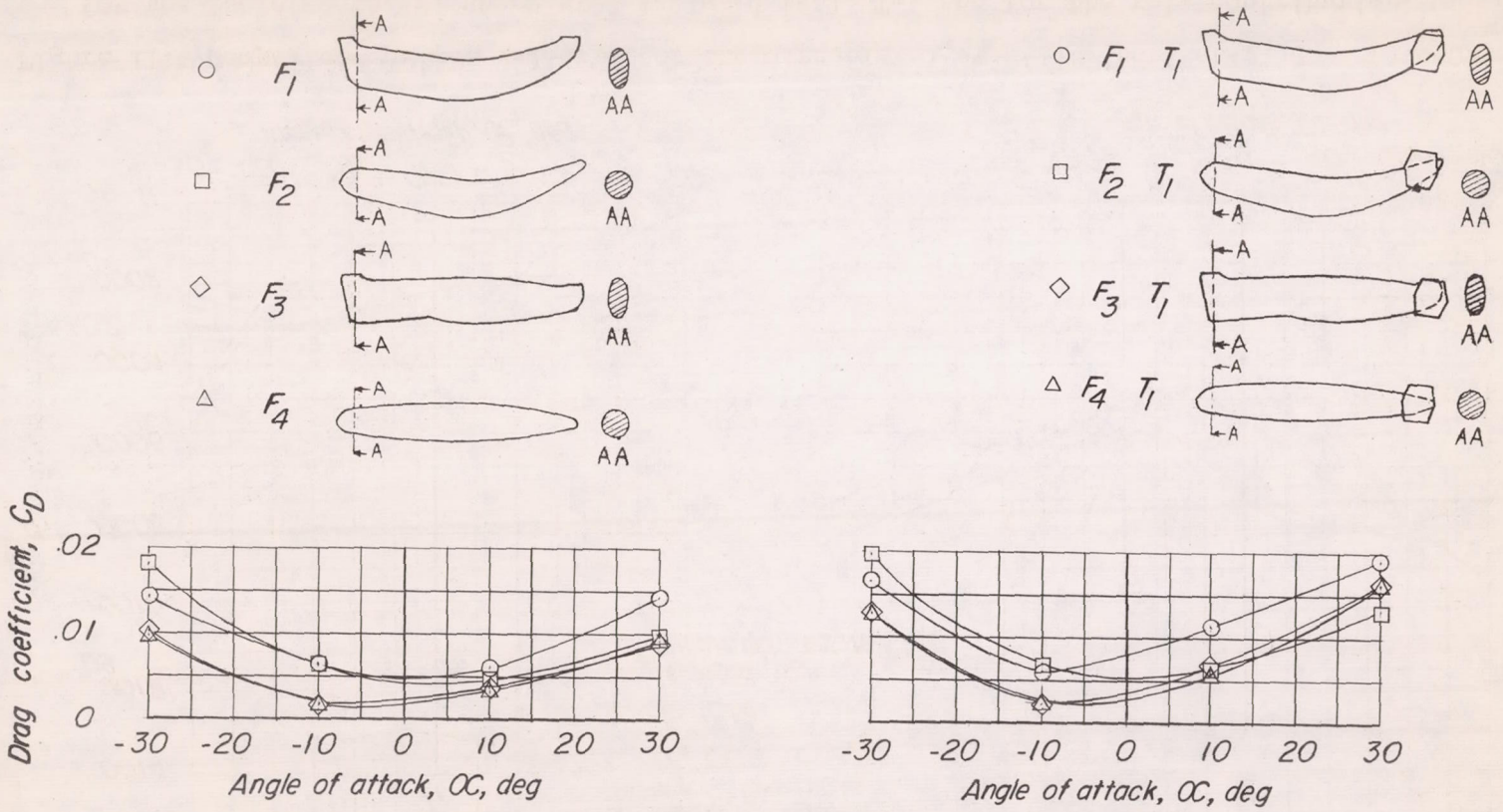


Figure 12.- Variation of drag coefficient with angle of attack ($\beta = 0$) for the fuselages with and without $T_1$.

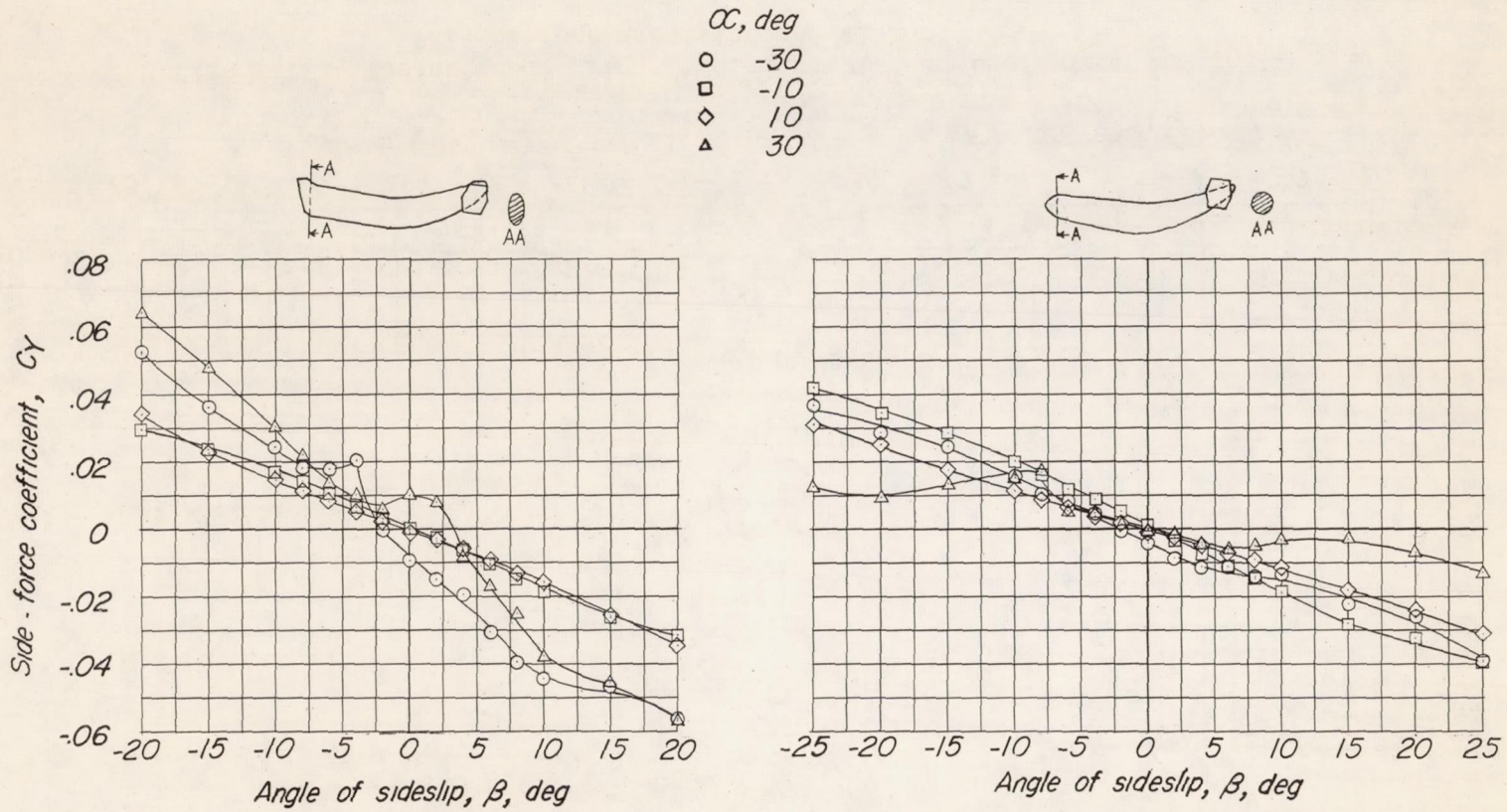


(a) Configuration $F_1T_1$.

(b) Configuration $F_2T_1$.

Figure 13.- Side-force characteristics in sideslip at several angles of attack for various configurations of a nonoverlap-type helicopter fuselage model.

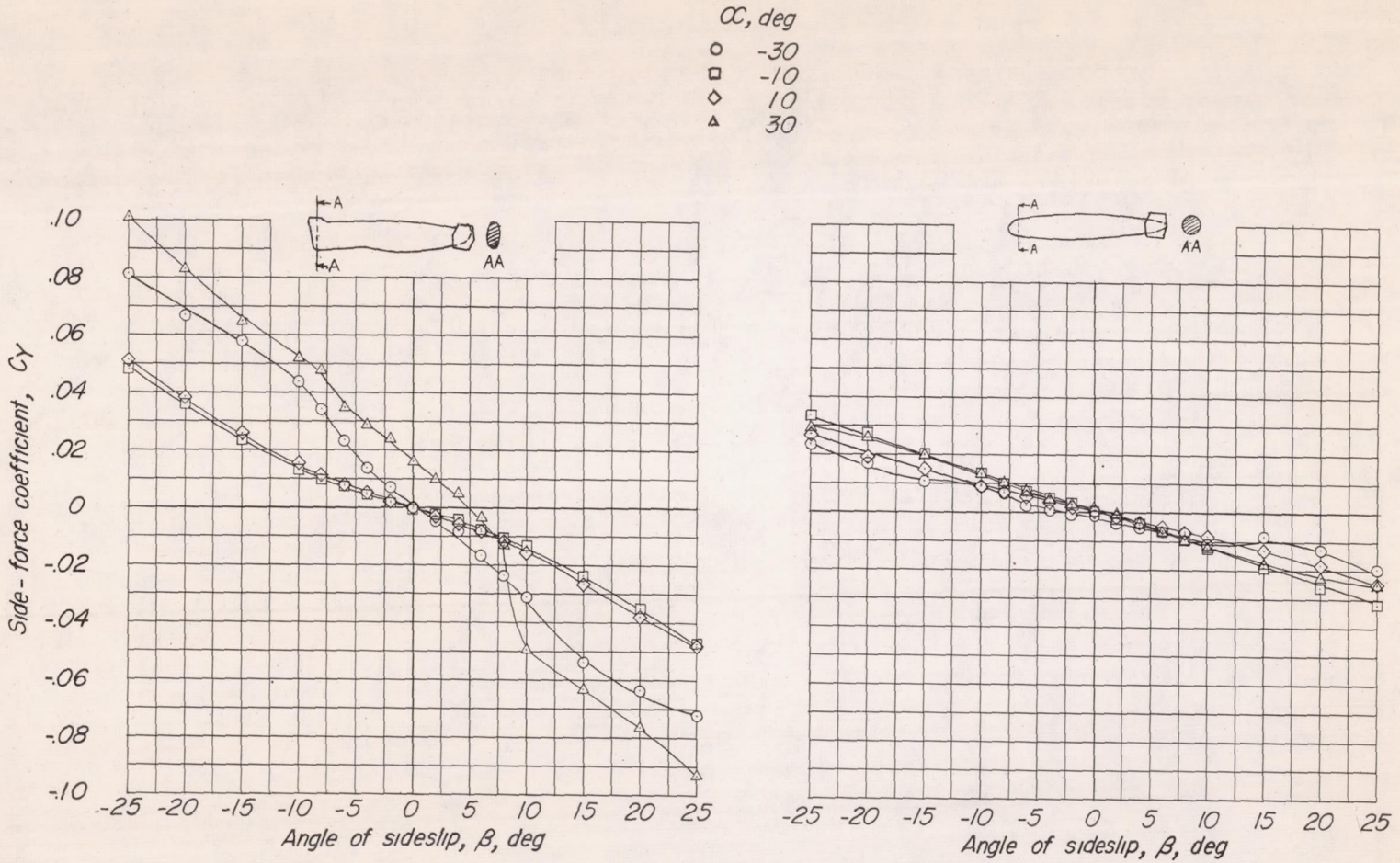


(c) Configuration $F_3T_1$.

(d) Configuration $F_4T_1$.

Figure 13.- Concluded.

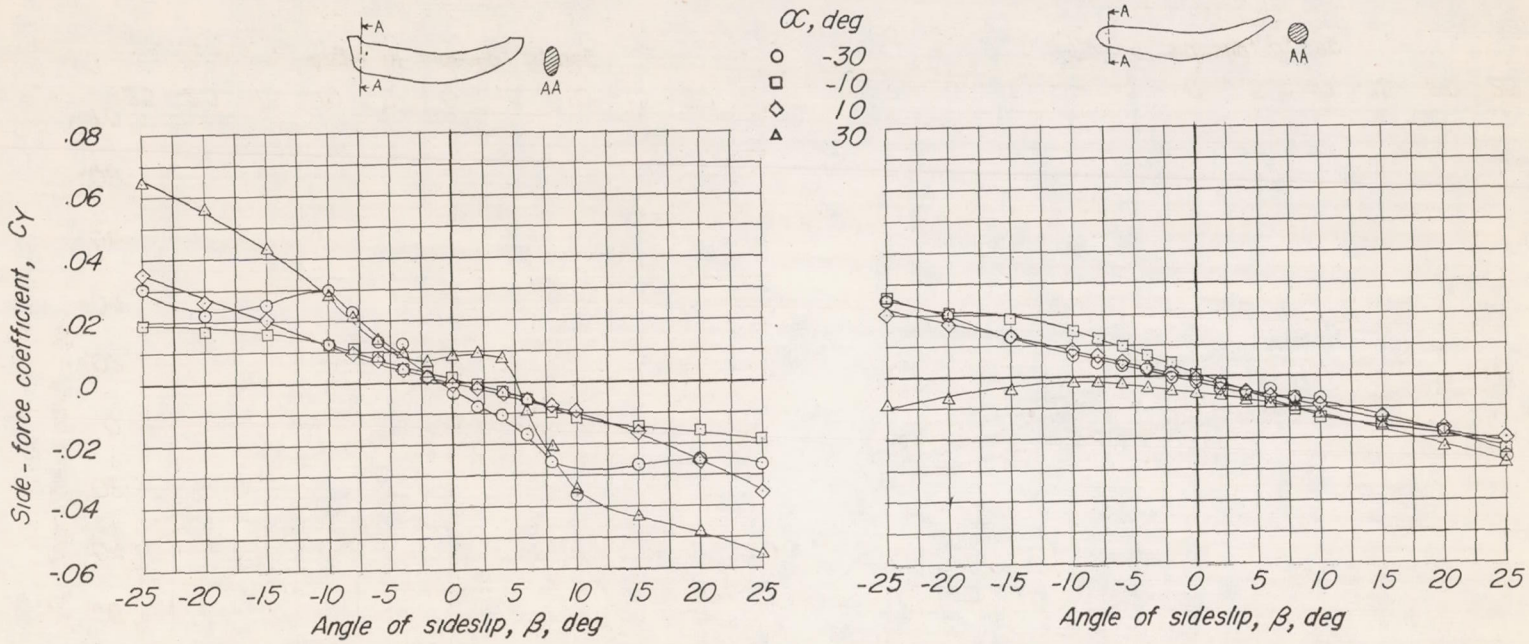


(a) Configuration $F_1$.

(b) Configuration $F_2$.

Figure 14.- Side-force characteristics in sideslip at several angles of attack for various configurations of a nonoverlap-type helicopter fuselage model.

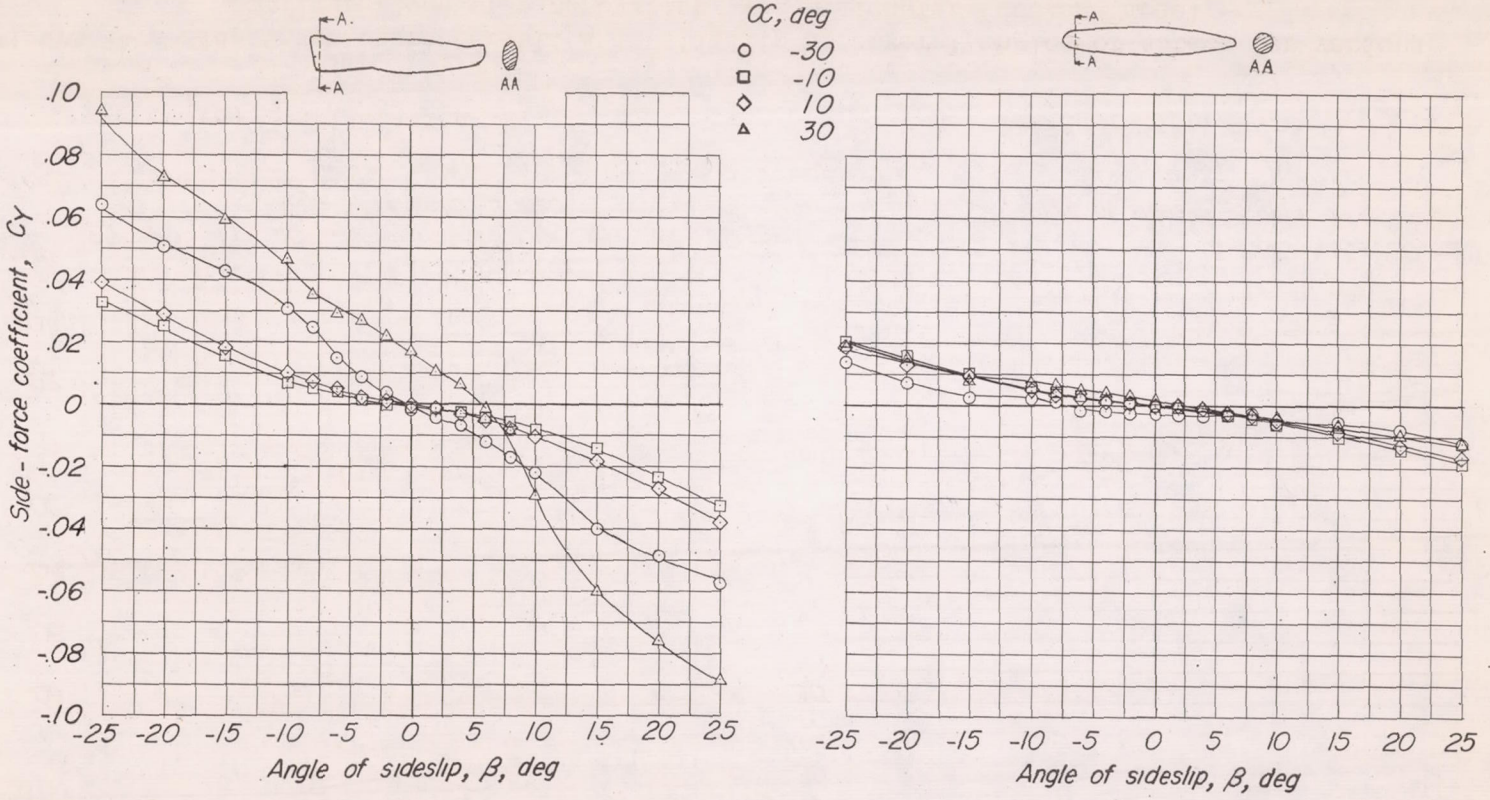


(c) Configuration $F_3$.

(d) Configuration $F_4$.

Figure 14.- Concluded.

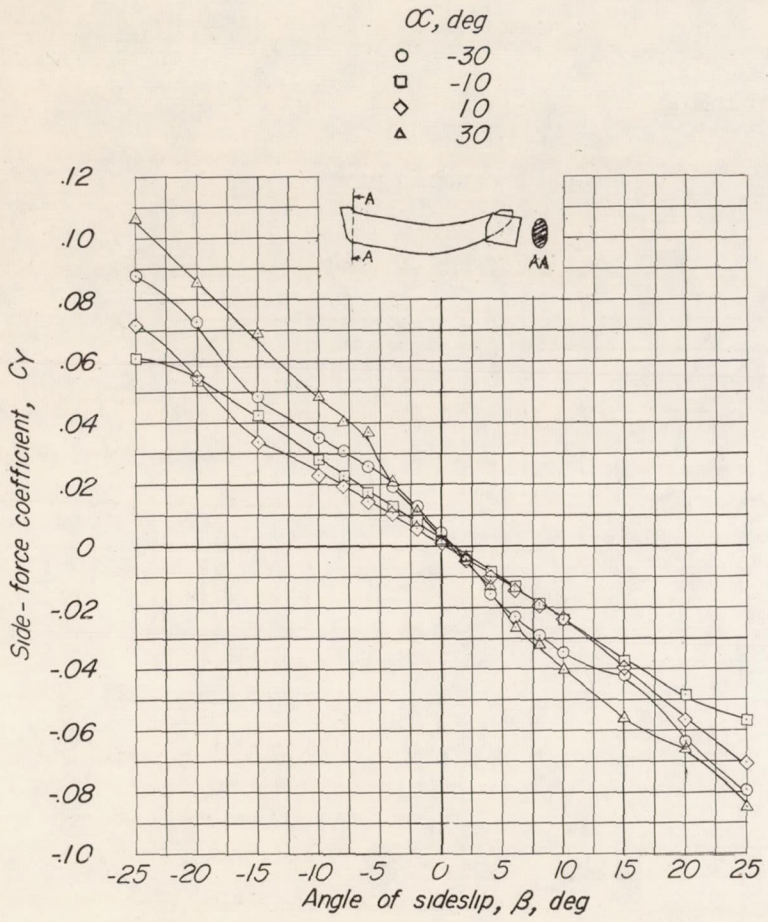


(a) Configuration $F_1T_2$.

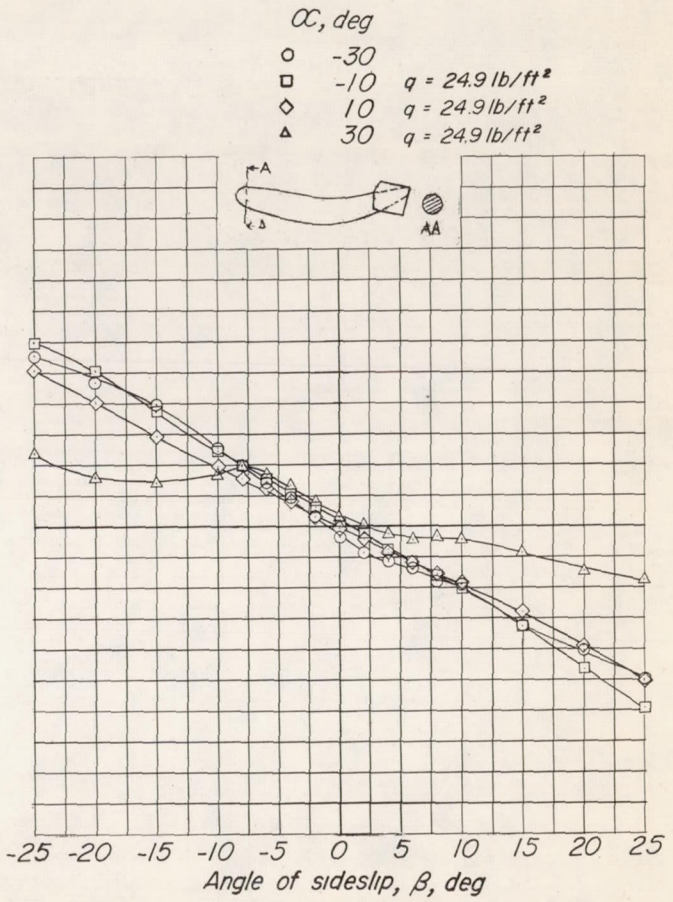


(b) Configuration $F_2T_2$.

Figure 15.- Side-force characteristics in sideslip at several angles of attack for various configurations of a nonoverlap-type helicopter fuselage model.

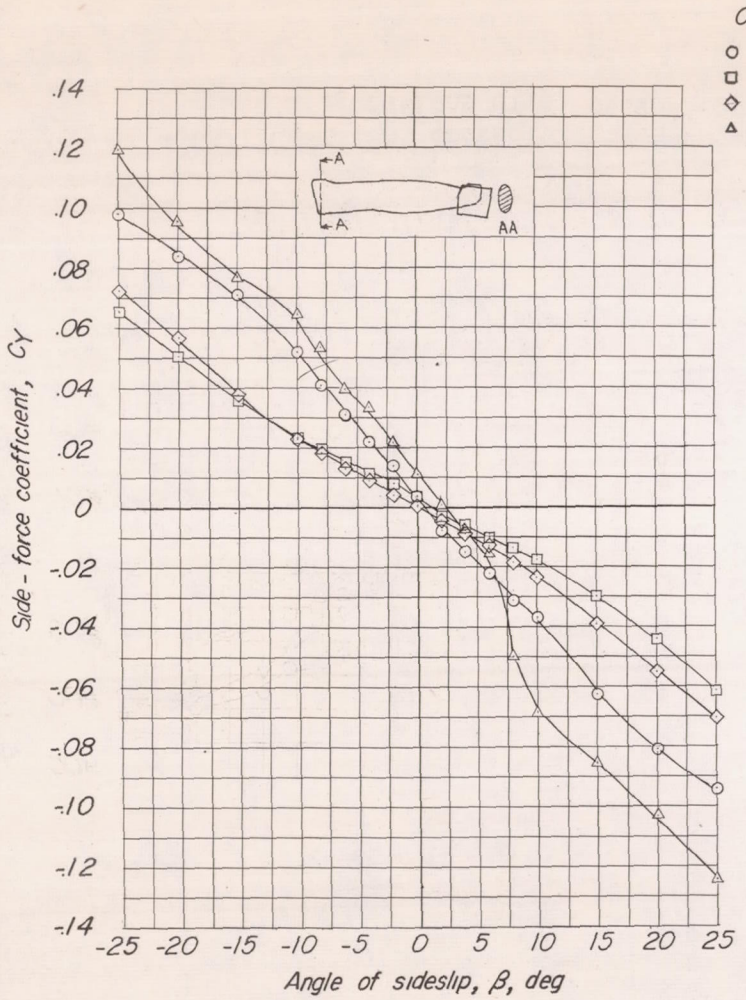


(c) Configuration $F_3T_2$.

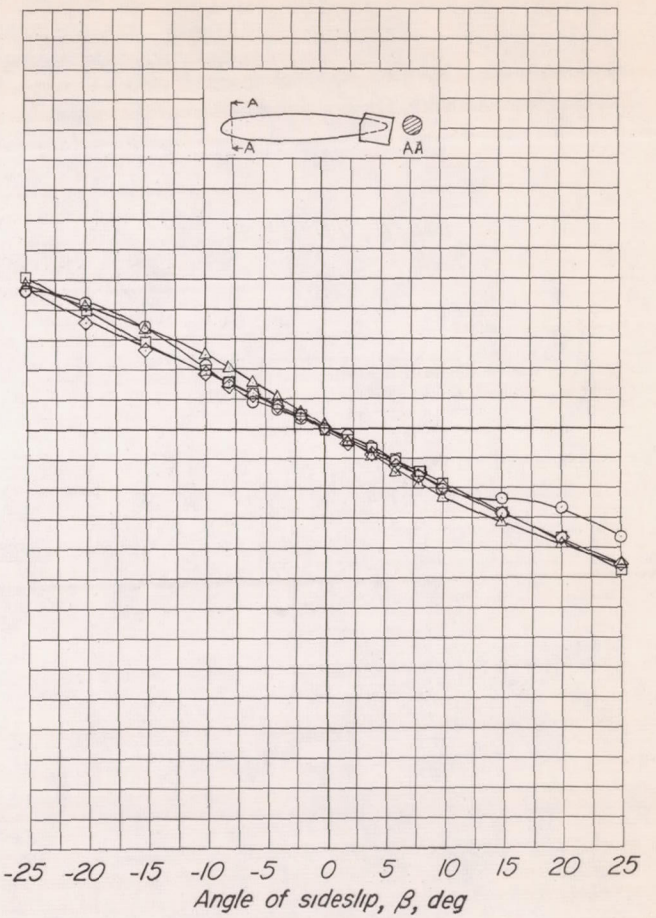


(d) Configuration $F_4T_2$.

Figure 15.- Concluded.

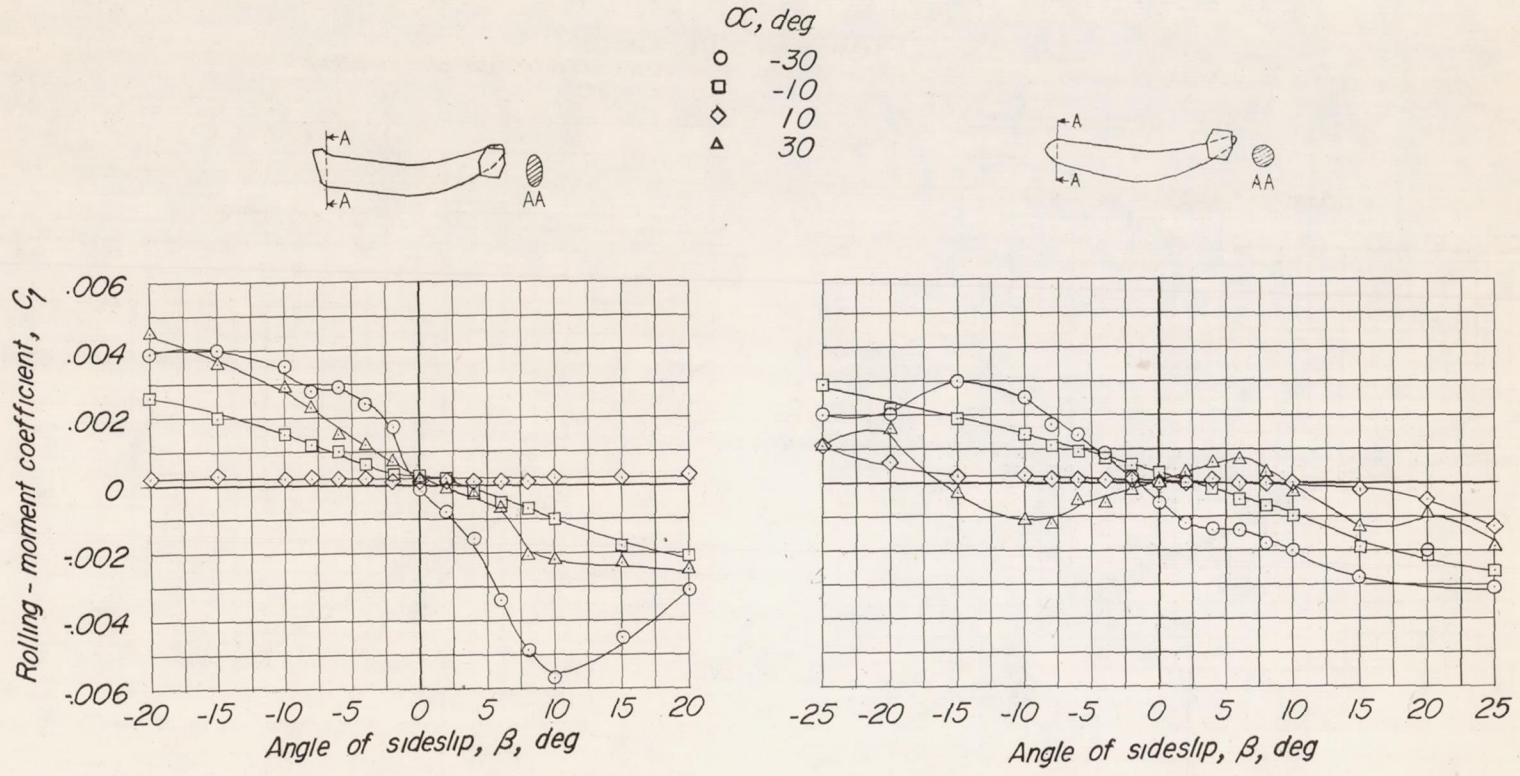


(a) Configuration $F_1T_1$.

(b) Configuration $F_2T_1$.

Figure 16.- Rolling-moment characteristics in sideslip at several angles of attack for various configurations of a nonoverlap-type helicopter fuselage model.

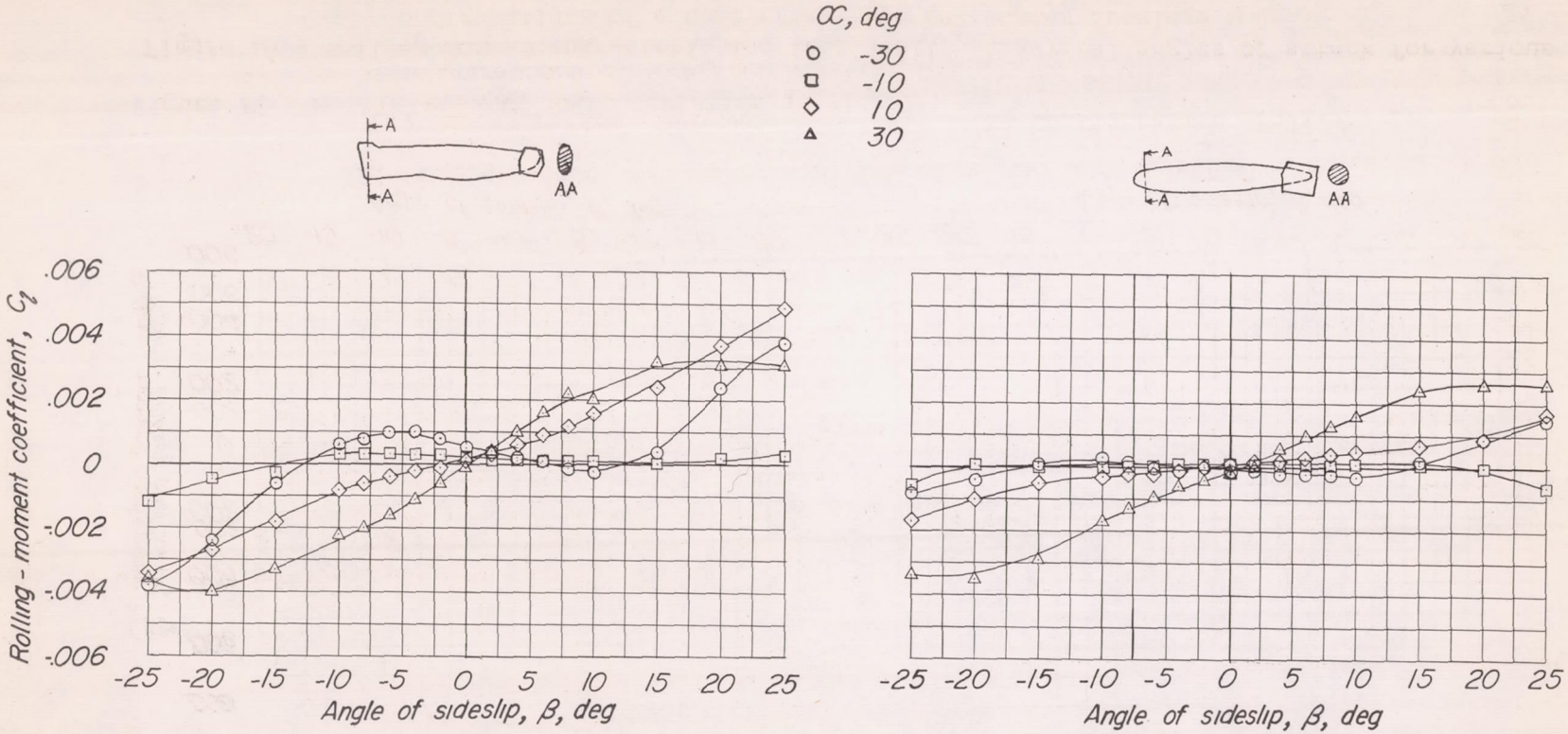


(c) Configuration $F_3T_1$.

(d) Configuration $F_4T_1$.

Figure 16.- Concluded.

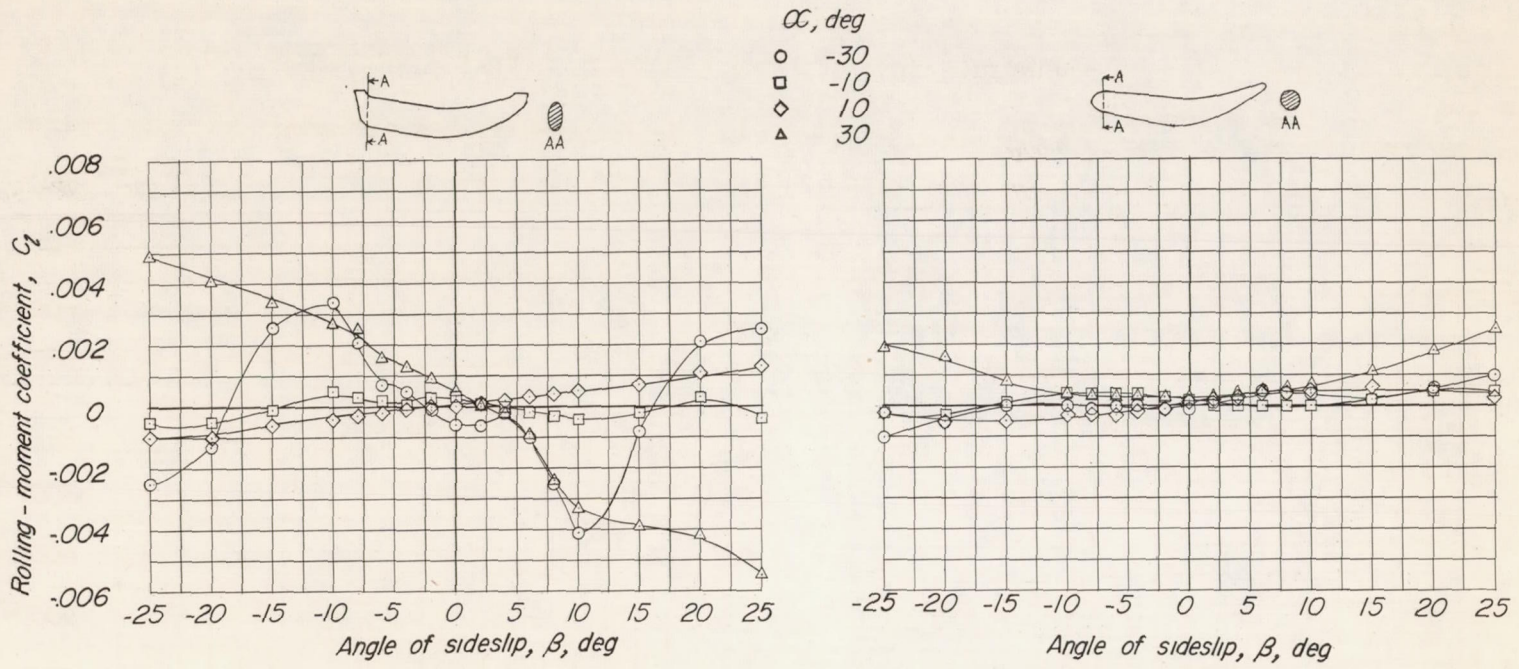


(a) Configuration $F_1$.

(b) Configuration $F_2$.

Figure 17.- Rolling-moment characteristics in sideslip at several angles of attack for various configurations of a nonoverlap-type helicopter fuselage model.

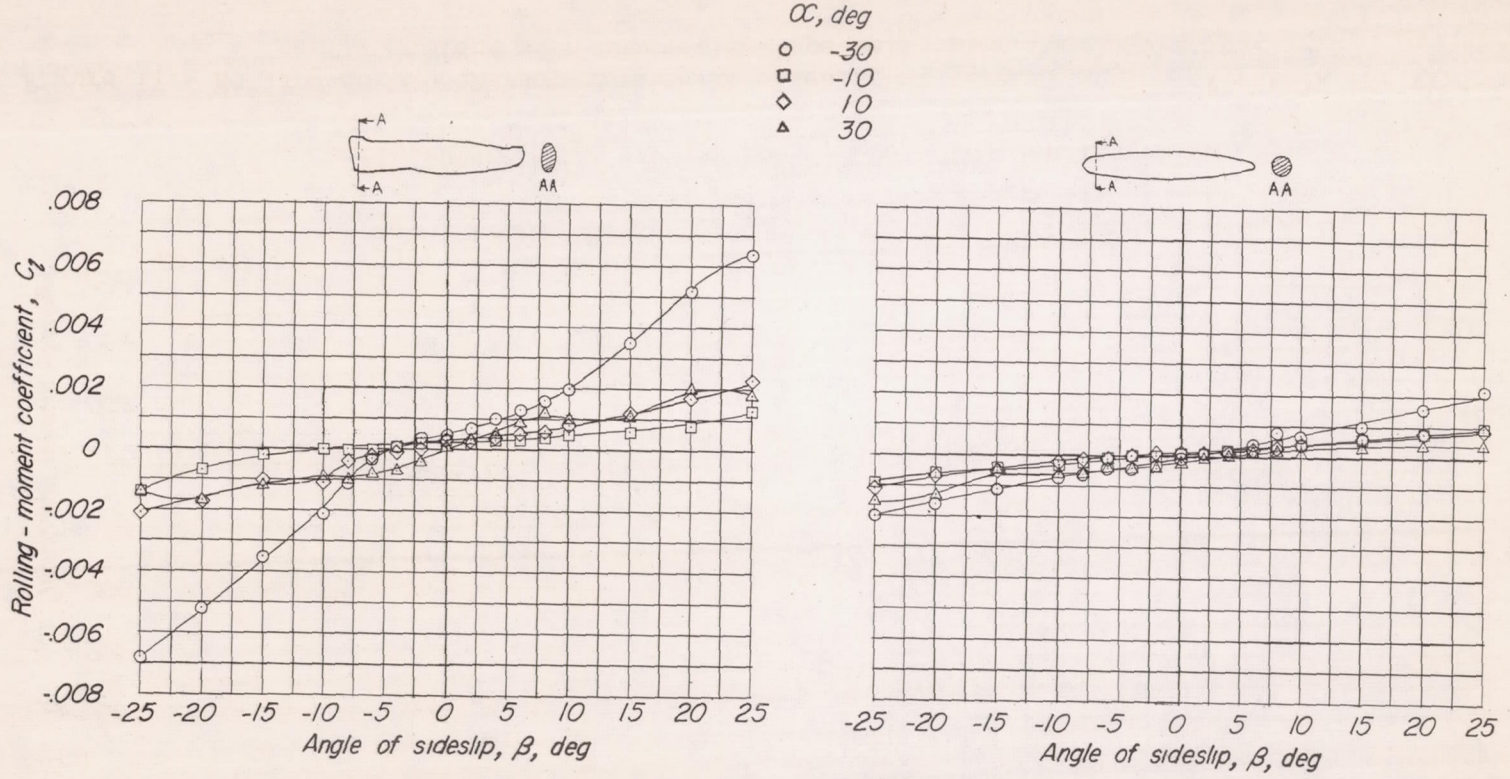


(c) Configuration $F_3$.

(d) Configuration $F_4$.

Figure 17.- Concluded.

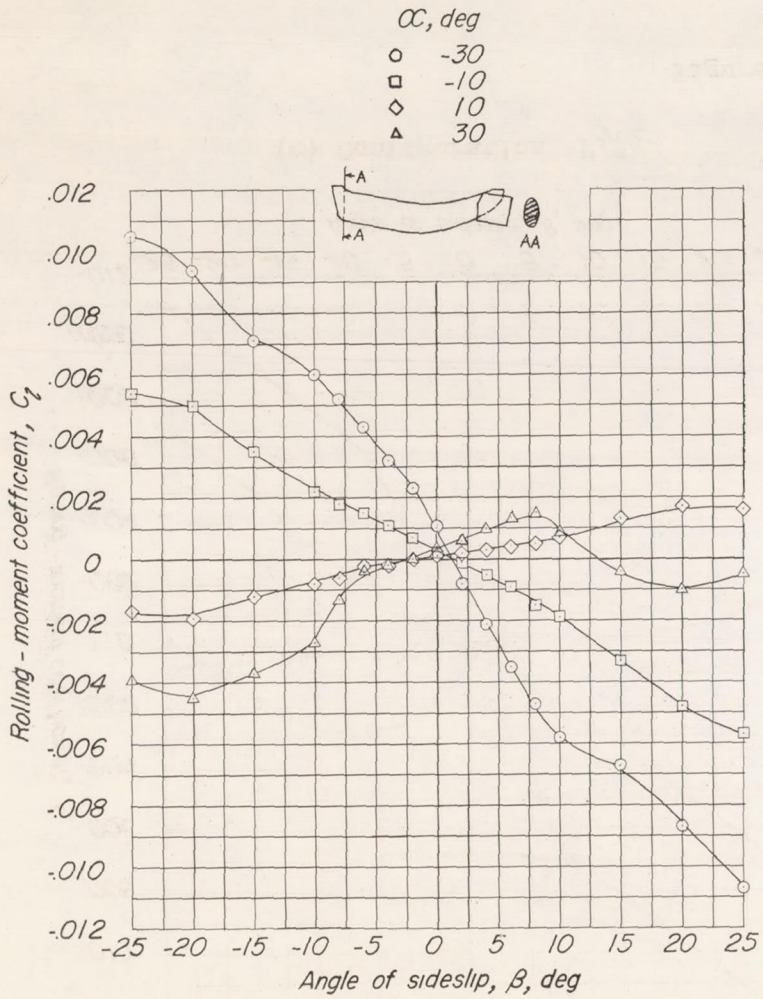


(a) Configuration $F_1T_2$.

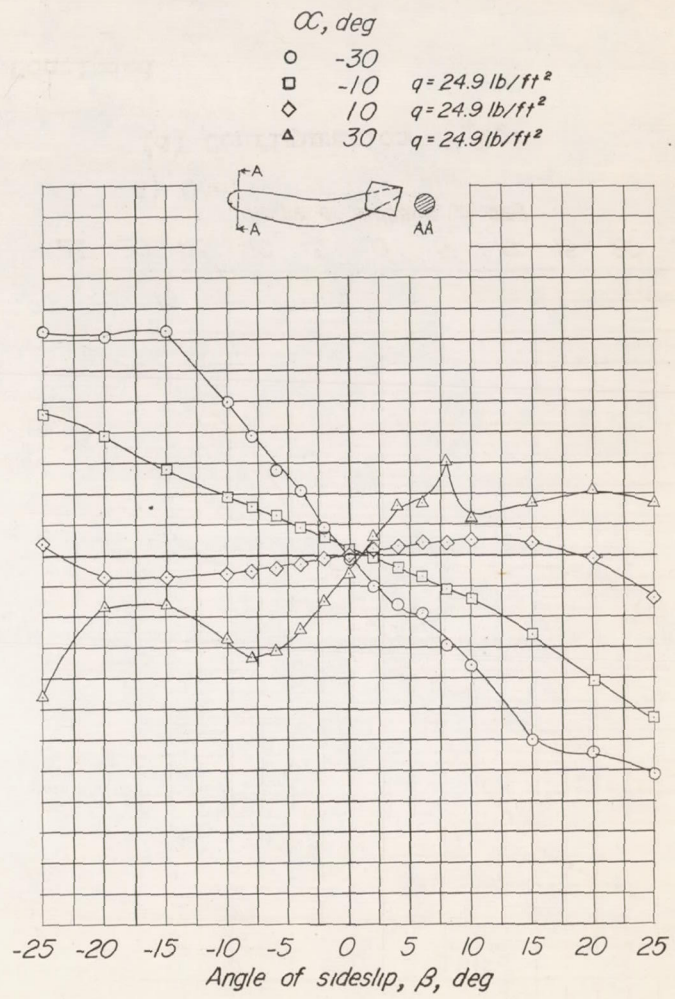


(b) Configuration $F_2T_2$.

Figure 18.- Rolling-moment characteristics in sideslip at several angles of attack for various configurations of a nonoverlap-type helicopter fuselage model.

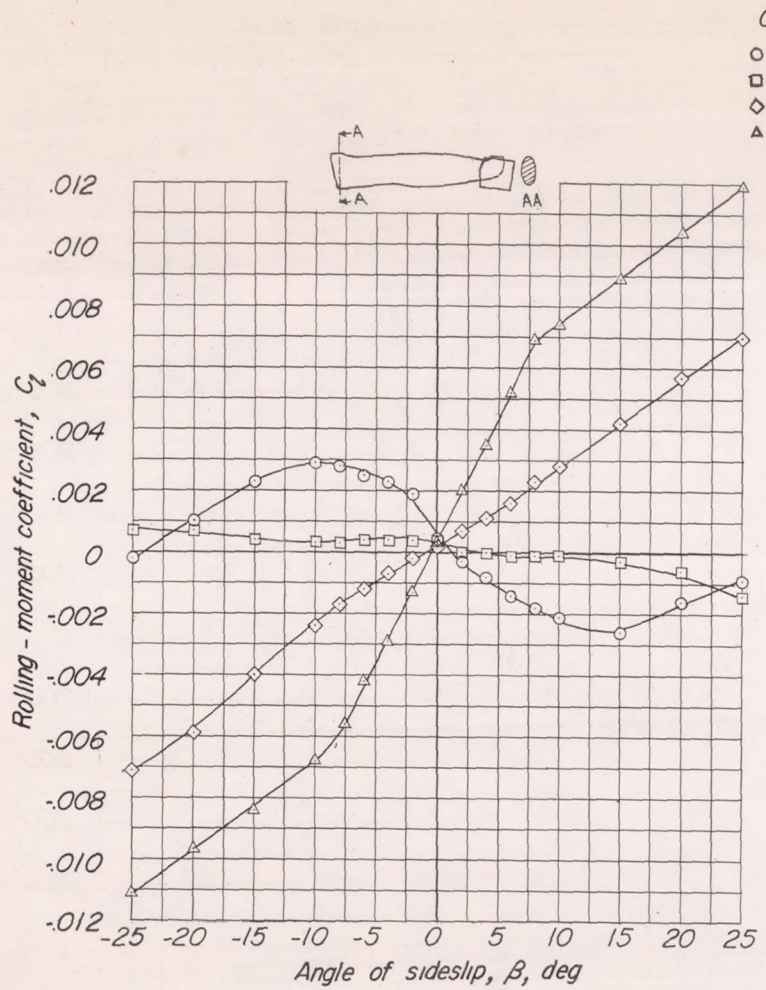


(c) Configuration $F_3T_2$.

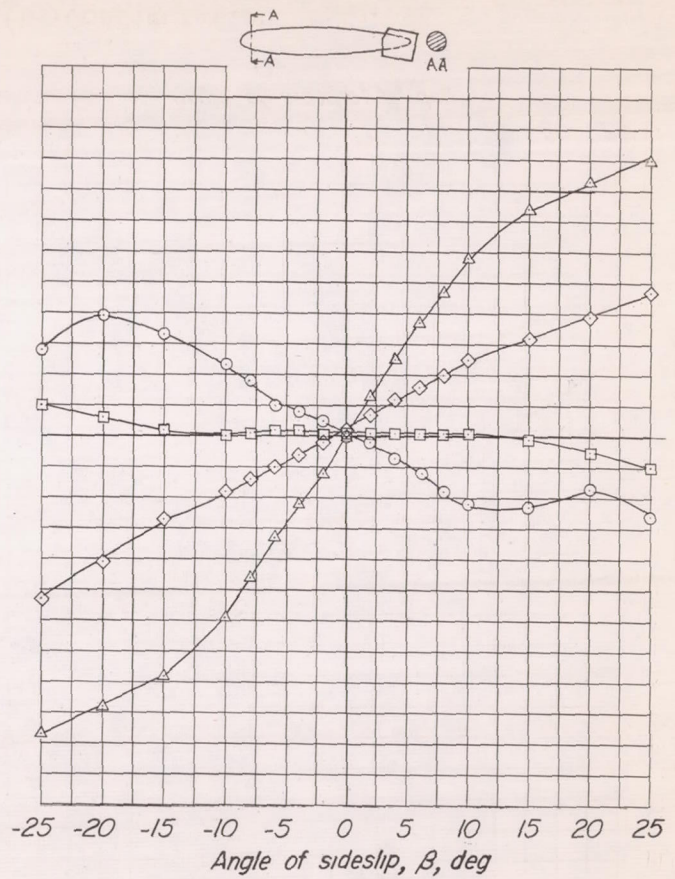


(d) Configuration $F_4T_2$.

Figure 18.- Concluded.